ARTIFICIAL NEURAL NETWORK MODELS UTILIZE CHAMBER-SPECIFIC PREDICTORS OF CARDIAC FIBROSIS IN OVARIECTOMIZED AND AORTIC-BANDED YUCATAN MINI-SWINE

A Thesis

Presented to

The Faculty of the Graduate School

At the University of Missouri-Columbia

By AMIRA AMIN

Dr. Craig Emter and Dr. Emily Leary, Thesis Supervisors

MAY 2022

The undersigned, appointed by the dean of the Graduate School, have examined the thesis entitled

ARTIFICIAL NEURAL NETWORK MODELS IDENTIFY CHAMBER-SPECIFIC PREDICTORS OF CARDIAC FIBROSIS IN OVARIECTOMIZED AND AORTIC-BANDED YUCATAN MINI-SWINE

Presented by Amira Amin, a candidate for the degree of Master of Biomedical Sciences,

and hereby certify that, in their opinion, it is worthy of acceptance.

Associate Professor Craig Emter

.....

Assistant Professor Emily Leary

.....

Associate Professor Kevin Cummings

.....

Dedication

This thesis is dedicated to:

My father who I know is watching over me now.

My family and friends who have always believed in me.

Every person who gave me a word of encouragement and kindness to help me get over a hard day

The seven-year-old me who believed I can do this based on nothing but dreams and hard work … Here we are.

Acknowledgement

Throughout the writing of this dissertation I have received a great deal of support and assistance. I would first like to thank both my supervisors, Dr. Emily Leary and Dr. Craig Emter, whose assistance and expertise was invaluable in guiding the research questions, methodology and learning throughout my Master's course. Your feedback and support always inspired me to work to a higher level and I aspire to keep improving. You are truly role models for me and I consider it a main opportunity in life to be your student.

I would like to acknowledge my colleagues from Emter lab for their collaboration. In addition to the support of biomedical science department who have always provided me with the tools that I needed to choose the right direction in my studies. I would like to single out Dr. Kevin Cummings who haves supported me even before I arrived in the United States. It's always reassuring for us as student to know that we can ask for help and find it and I hope our performance reflects your efforts.

In addition, I would like to thank my sponsoring scholarship for giving me this opportunity to learn as a researcher and as a human.

Table of contents

List of figures

List of Tables

List of equations

List of Abbreviations

HF	Heart failure
HFpEF	Heart failure with preserved ejection fraction
HFrEF	Heart failure with reduced ejection fraction
HFmrEF	Heart failure with midrange ejection fraction
LVEF	Left ventricular ejection fraction
LV	Left ventricle
RV	Right ventricle
BNP	B-type natriuretic peptide
NT-proBNP	N-terminal pro-BNP
ECM	Extra cellular matrix
FN	Fibronectin
RVEF	Right ventricular ejection fraction
ML	Machine learning
ANN	Artificial Neural Networks
AI	Artificial intelligence
AUC	Area under the curve
AB	Aortic banding
OVX	Ovareictomy
CON	Control (non- aortic banding)
INT	Intact (non-ovareictomy)
TCC	Total collagen content
MMP	Matrix metalloprotease

IMP	Tissue inhibitor of Matrix metalloprotease
ERK	Extracellular signal-regulated Kinase
DUSP	Dual-Specificity Phosphatase
JNK	c-Jun Amino-Terminal Kinases
MAPK	Mitogen activated protein Kinase
MAPKK	Mitogen activated protein Kinase Kinase
ESR	Estrogen Receptor 1
PGR	Progesterone Receptor
PGRMC1	progesterone receptor membrane component 1
MAP	Mean Arterial Pressure
TGFβ	Tumor growth factor β
RAAS	Renin Angiotensin Aldosterone system

Abstract

Objective: Heart failure with preserved ejection fraction (HFpEF) is a disease associated with significant clinical pathophysiological heterogeneity in which maladaptive cardiac fibrosis, in both the right and left ventricles of the heart, plays a unique role in the manifestation of disease. Fibrotic remodeling quantified in this project occurs in a chamber-dependent manner on both sides of the heart. Extracellular matrix (ECM) remodeling is the core of this pathological process. The prevalence of HFpEF is greater in postmenopausal women with hypertension. Therefore, the goal of this study was to assess the role of female sex hormones on chamber-dependent differences i.e., left ventricle (LV) vs. right ventricle (RV), in ECM remodeling and regulation in a mini-swine model of pressure overload-induced heart failure (HF). To gain insight about the regulation of fibrosis in this model, biological inputs were measured in both the right and left ventricles and used as input variables in an artificial neural network model (ANN). This model will identify best predictors for experimental group status i.e., the combination of the loss of female sex hormone and/or pressure overload status, as an indication for the biological roles they play in the fibrotic remodeling process.

Hypothesis: I hypothesized molecular markers involved in the bioregulation of the cardiac ECM can predict experimental group status in a chamber-specific manner.

Methods:

a) Animal model: An ovariectomy (OVX) model of surgically induced menopause was used to model the loss of female sex hormones. Separately, aortic banding (AB) was used to induce pressure-overload and mimic HFpEF. Animals that did

not undergo ovariectomy were assigned to the intact (INT) groups and animals that did not undergo AB were assigned as control (CON).

b) Data: 24 six month old female swine were categorized into 4 groups by ovariectomy and aortic-banded status: 1) Control, intact (CON-INT; n=6); 2) CON-OVX (n=5); 3) AB-INT (n=7) ;and 4) AB-OVX (n=6).

c) Ninety-six biological measurements from both the LV and RV were considered including different mRNA, proteins, activity and/or abundance levels of various extracellular matrix components including structural proteins and regulatory pathways.

d) Data preprocessing: Missing data were mean imputed and the min-max normalization method was used for all measures. One-way ANOVA models were used to identify mRNA or protein targets associated with group status for consideration in the ANN. Data were split into testing and training sets with one observation from each group (n=4 total) retained for later model testing i.e., 84% training and 16% testing

e) Artificial neural network model: Measurements associated with group status were then used as input features in the ANN model. Multiple activation functions were considered. Different combinations of hidden layers and nodes within each layer were optimized. Cross-validation, confusion matrices, and F1 scores, percentage accuracy and balanced accuracy for each experimental group were used to describe the accuracy of the developed ANN model.

Results: One-way ANOVA models indicated that in the LV, total collagen content, TIMP-1 mRNA, total JNK protein level, MMP-14 activity, MMP-2 activity and

collagen I mRNA were associated with group status ($p<0.1$). In the RV, total collagen content and collagen I and III mRNA levels were associated with group status ($p<0.1$). These nine molecular markers were used to develop the ANN model. Cross-validation and confusion matrices indicate all nine targets formed a linear relationship predictive of group with an overall accuracy of 70.7% and F1 score of 0.81.

Conclusion: Molecular mechanisms involved in the bioregulation of the ECM have analytical power to determine sex hormone and aortic-banding status in a pre-clinical model of pressure overload-induced HF. These findings indicate that nine biological measures could predict experimental group status in our pre-clinical swine model. Therefore, I identified these variables as potential biomarkers of fibrotic remodeling in a HFpEF phenotype with loss of female sex hormones and pressure overload. I also highlight the importance of these nine variables in the fibrotic remodeling process on both sides of the heart.

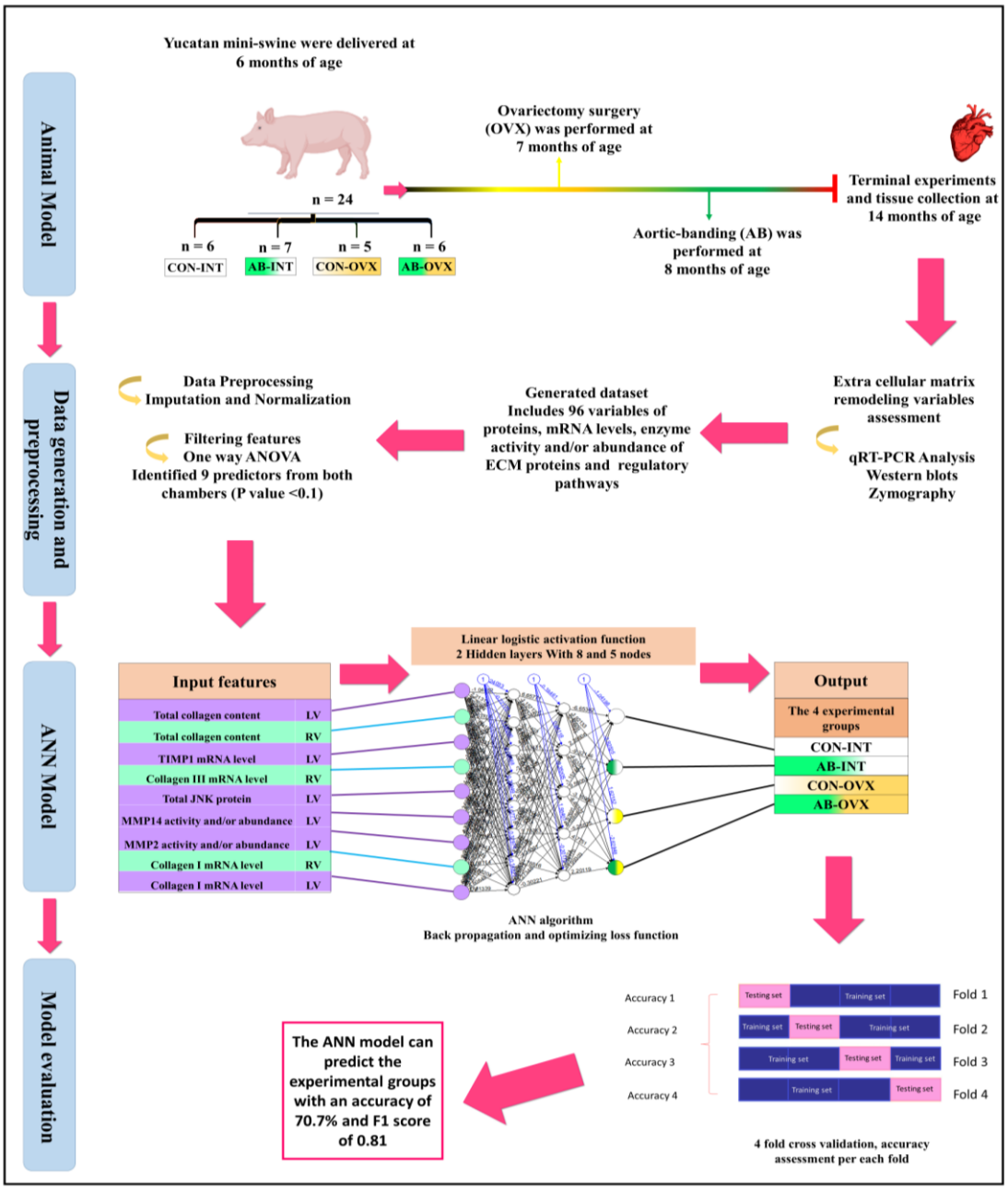

Figure 1-1: Overall study outline illustrates animal model and fibrotic remodeling assessment and artificial neural network model building and evaluation. Acronyms: CON-INT; Control-intact, AB-INT; Aortic banded-Intact, CON-OVX; Control-ovariectomized, AB-OVX; Aortic bended-ovariectomized, MMP2; Matrix metalloprotease 2, MMP14, Matrix metalloprotease 14, TIMP 1; Tissue inhibitor of matrix metalloprotease 1, JNK; c-Jun Amino-Terminal Kinases, LV; Left ventricle, RV; Right ventricle, ANN; Artificial neural network.

CHAPTER I: INTRODUCTION TO HEART FAILURE AND MACHINE LEARNING IN BIOMEDICAL SCIENCES

Heart failure with preserved ejection fraction: scattered pieces of the puzzle

Heart failure (HF) is an ongoing epidemic that is responsible for substantial mortality rates, health care resource utilization, and poor quality of life.[1] In the United States, heart failure is the most frequent cause for hospitalization.[2] Among the different markers used for diagnosis of heart failure, left ventricular ejection fraction (LVEF) was established as a phenotypic marker to explain the unique pathophysiological changes and responsivity to therapeutic regimens among HF patients. Therefore, a LVEF based criteria divides HF patients into three categories; heart failure with reduced ejection fraction (HFrEF) with LVEF ≤40% which is characterized by overt systolic dysfunction, heart failure with mid-range ejection fraction (HFmrEF) LVEF 41–49%% and heart failure with preserved ejection fraction (HFpEF) LVEF ≥50%.[1,3,4] Over the past decade, evidence shows that the prevalence of HFrEF is decreasing, yet the proportion of HFpEF cases is significantly increasing.[5] The quality-of-life in HFpEF patients is on par or worse than HFrEF and their average levels of physical activity are similar to moderate-to-severe chronic obstructive pulmonary disease.[6] It is critical that more research should focus on HFpEF in attempt to answer these questions, which I summarize here.

Heart failure with preserved ejection fraction (HFpEF) is a major cardiovascular issue that is arguably the biggest unmet need in cardiovascular medicine.[7] HFpEF accounts for 50% of all HF patients and the prevalence is increasing with increasing rates of obesity, diabetes and an aging population. Generally, heart failure is diagnosed based on common signs and symptoms, which may be identified by structural or functional abnormalities using chest X-ray or echocardiography.[7,8] Potential underdiagnoses of HFpEF is suspected based on the overlap of the symptoms between heart failure patients coupled with the lack of consistent diagnostic criteria due to pathological and phenotypical heterogeneity of HFpEF.[9]

Various hypotheses have been proposed for the pathogenesis of the multifactorial nature of HFpEF. Circulating inflammatory biomarkers including interleukin- 1, tumor necrosis factor- alpha and C- reactive proteins are higher in HFpEF than HFrEF. [10,11] Compared to the inflammatory state in HFrEF characterized by factors including ischemia induced necrosis, acute trauma, blood volume loss, coronary artery disease or limited number of infections, the inflammatory state in HFpEF remains misunderstood. The etiology of the systematic inflammatory state in HFpEF is not limited to a number of factors mainly affecting cardiovascular system but it includes pulmonary, vascular, renal, liver disease and metabolic syndrome affecting a broad range of systems and biological functions.[12] These multi-organ functions are altered in each patient such that various combinations manifest different phenotypes across heterogeneous groups of patients. In addition to the inability to determine the temporal sequence of pathogenic events, this heterogeneity makes HFpEF more challenging to understand. Consequently, effective treatments for HFpEF are limited.[13]

For example, assessment of for B-type natriuretic peptide (BNP) or N-terminal pro-BNP (NT-proBNP) is one of the main diagnostic tools used to assess heart failure. However, BNP and NT-proBNP vary among known HFpEF phenotypes. Obese HFpEF patients typically show normal levels of each, consistently below the threshold for heart failure diagnosis. However, atrial fibrillation – present in 30% of HFpEF patients – is associated with high BNP, levels regardless of HFpEF status.[14] To add to the complexity of HFpEF, a number of predisposing risk factors exist, specifically, female sex and older age are the most consistently reported.

Age- and sex-specific prevalence of HFpEF in European individuals greater than 80 years of age is approximately 8–10 % in women and 4–6 % in men.[5,15,16] Further, the risk for HF incidence at older age is decreasing for HFrEF but the same trend is not seen in HFpEF. Some argue that the sex discrepancy is not as pronounced as previously reported, given that age is considered the dominant risk factor for HFpEF and in statistics from 2012, 60% of the US population aged ≥75 years were women.[17] The gap between the male to female ratios widen with increasing age. In statistics from 2016 in the US, the ratio between males and females between 65 and 74 years of age was 79 male for every 100 females. In the age group above 85 years of age, there was only 53 males for each 100 females.[18]

However, previous clinical studies suggested a linkage between female sex hormones and the development of a profibrotic phenotype.[17,19,20]

In summary, HFpEF is major cardiovascular challenge due to multifactorial nature of the disease, the increasing prevalence, poor quality of life and prognosis across patients, lack of effective treatment, and failure of the currently available treatment of other

cardiovascular problems like HFrEF to show any efficacy. Better understanding of the pathogenesis towards the development of diagnostic and predictive tools for clinical management is needed. Regarding this broad goal, we aim to focus on a particular part of the pathogenesis, the maladaptive cardiac fibrotic remodeling in HFpEF.

Fibrotic remodeling in heart failure with preserved ejection fraction

Among the many factors contributing to the pathogenesis of HFpEF, fibrotic remodeling plays a unique role in the manifestation of the HFpEF. It has been established that fibrotic remodeling is correlated to the development of one of the most common HFpEF hallmarks, diastolic dysfunction.[21] Pathological fibrotic remodeling contributes to passive ventricular stiffness and reduced compliance, impairment of myocardial relaxation, and to the overall diastolic dysfunction.[22] Fibrotic remodeling is also correlated to higher hospitalization and mortality rates in HFpEF patients, compared to control subjects in the same age and sex categories.[23] During the early development phases of HFpEF, this type of interstitial diffuse fibrotic remodeling is among the significant structural changes in the heart that accumulates over time without overt symptoms until the development of HFpEF. This makes reversing or slowing fibrotic changes an attractive target to ameliorate HFpEF symptoms.[24,25]

Fibrotic remodeling is the quantitative and qualitative changes in collagen synthesis, degradation and deposition that determine the biomechanical properties of extracellular matrix (ECM) in the myocardium. Extracellular matrix is a dynamic network composed of fibrous protein, glycosaminoglycan, and glycoconjugate that plays a fundamental role in maintaining myocyte orientations, structural integrity, and myocardial adaptation to any stress; hence, mediating pathological structural remodeling. [26]

For the heart, the two main collagen subtypes are collagen I, accounting for 85-90% of total collagen, and collagen III, accounting for 5 to 10%. Other subtypes comprise a small percentage for the remaining collagen. In pathological conditions like HFpEF, the ratio between the collagen subtypes changes such that the less compliant collagen I ratio to the more elastic collagen III ratio increases, playing a role in diastolic dysfunction development.[27,28]

Fibronectin (FN) is another component in the extracellular matrix microenvironment that plays an essential role in controlling cell-cell and cell-matrix adhesion through integrins receptor bindings. In addition, FN has a protective role regulating fibrillary collagen and extracellular and intracellular communication. [29] Fiber stretch-assay studies revealed that collagen I's FN-binding domain is responsible for a mechano-regulated interaction between the two proteins. Relaxed FN fibers are required for collagen 1 assembly but once assembled, collagen 1 fibers act as shield for FN fibers from cellular traction force.[30,31] Fibronectin polymerization is necessary for collagen deposition and fibrotic remodeling incidence. Therefore, fibronectin remodeling and interaction with collagen has been suggested as a target to alleviate fibrotic remodeling in the heart.[32] Interstitial fibrotic remodeling is a unique form of fibrosis in which collagen-rich ECM deposits in the interstitial space between cells. This type of remodeling is most commonly associated with abnormal loading conditions on the heart.[33]

In a remarkable resemblance to the complicated nature of HFpEF, fibrotic ECM remodeling as a part of the pathogenesis shows a complex nature that integrates multiple factors from different physiological levels. Despite the essential role played by cardiac fibroblasts in fibrotic remodeling, recent studies of metabolic diseases indicate that an

increase in ECM synthesis could occur in the absence of cardiac fibroblast activation.[34,35] In addition, multiple molecular pathways are known to provide profibrotic signals including Tumor growth factor β (TGFβ), Renin Angiotensin Aldosterone system (RAAS) through Angiotensin II receptors in addition to mineralocorticoids and sex hormone receptors that activate downstream pathways.[36–39] These pathways activate a cascade of kinases and phosphatases that affect ECM remodeling among other downstream targets. In this work I highlight the role of Mitogen Activated Protein Kinases (MAPK) including the extracellular signal-regulated kinase (ERK), c-Jun N-terminal kinase (JNK) and Dual activity Phosphatases (DUSP) that collectively add another layer of regulation on ECM. [40,41]

Extracellular matrix regulation

Extra cellular matrix (ECM) protein synthesis and degradation falls under the tight regulation of a complex network of proteins and regulatory enzymes amongst which matrix metalloproteases (MMPs) and their inhibitors (tissue inhibitor of matrix metalloprotease or TIMPs) play an indispensable role in ECM protein homeostasis and fall under the regulation on the previously described kinases.[42] MMPs are a family of proteolytic enzymes that regulate the degradation of ECM and inflammatory signaling. MMPs share a common structural framework acting on ECM substrates like collagen subtypes and fibronectin according to their catalytic domain. These commonalities highlight significant overlap in their activities.[43] Their transcription is tightly regulated by bioactive molecules and mechanical stimuli in a constitutive or induced manner through multiple signaling pathways including the aforementioned MAPK, cJNK and ERK pathways.[43] TIMPs are specific inhibitors that digest and stop the proteolytic activity of

MMPs. The exact kinetics of this process and nature of different interactions between MMPs and TIMPs is not fully understood.[44] MMPs and TIMPs can also contribute to the expression, post transcriptional modification and/or activation of one another. Inflammatory signals like pro-inflammatory cytokines result in MMPs activation, however, long term activation increases TIMPS level in parallel to MMPs.[45] Various MMPs and TIMPs have been studied as predictive markers for the development of many cardiovascular diseases. Although multiple reviews indicate the potential importance of MMPs and TIMPs expression and activity levels as diagnostic or prognostic tools, data about the exact roles of MMPs and TIMPs in HFpEF is still lacking.[46]

Left ventricular diastolic dysfunction has been extensively studied in the setting of HFpEF. Diastolic dysfunction in the LV which is correlated with fibrosis, progress into increased LV end diastolic pressure which can be combined with left atrial remodeling showing overt HFpEF symptoms.[47] Looking into clinical studies results, right ventricle dysfunction imposes a significant importance in HFpEF pathogenesis as well.

A meta-analysis estimates that 18-28% of the overall HFpEF population show signs of right ventricular dysfunction which is associated with poor prognosis and more severe phenotypes. [48] Other studies indicate that right ventricular ejection fraction (RVEF) alone can be used as a predictor for survival in other cardiovascular diseases like congestive heart failure, unfortunately, this was not investigated in HFpEF. HFpEF patients with right ventricular dysfunction show higher natriuretic peptide levels, more severe pulmonary and coronary vascular disease, lower RVEF and more right ventricular stiffness. [49] In a clinical trial on HFpEF patients, right side heart failure was associated

with 91.4 % of all deaths due to cardiovascular causes. [50] Adding the risk of pulmonary hypertension and right side heart failure raises the mortality rates for HFpEF patients by ten fold.[47]

The focus of my thesis study shows an overt difference between the fibrotic remodeling process in the right and left ventricle. It was previously reported that the right ventricle collagen content is higher than left ventricle on a normal physiological level.[51] Yet, for other ECM components, a comparison was not conducted. Most studies investigating ECM composition and remodeling have focused on the LV. Relative to the ventricular size, the collagen content percentage in the right ventricle was more than twice the percentage in the LV. [51] On a healthy physiological level, cell-generated mechanical stresses of varying magnitude are exerted on ECM fibers on both sides of the heart leading to possible differences in the regulatory process for ECM assembly into an interwoven structure which is rarely studied.[52]

A machine learning approach for cardiology.

Machine learning (ML) can be defined as how computers make sense of data and make decisions or classify tasks with or without human supervision. The basic concept for the framework of most ML models is receiving input data (e.g., images, numerical values, or text) and, through a combination of mathematical optimization and statistical analysis, the model can predict outcomes, classify, or describe data.[53] Several ML models, or algorithms, have been applied in cardiovascular science to improve several available diagnostic tools, such as the electrocardiogram and echocardiogram. However, the clinical application of individual ML models remains limited.[54]

When considering the clinical application of any statistical tool for cardiology, the challenging nature of cardiovascular problems must be considered, such as that in HFpEF. Integrating data from various physiological levels, generated using different quantifying methods and systems, to make predictions or identify important factors and solutions is extremely challenging. The different phenotypes of HFpEF makes applying any model's outcomes on individual patients more complicated.[54–56]

In general, a standard statistical approach is to test a hypothesis and make conclusions from those results. When the hypothesis is a straightforward one, e.g. the existence of a type of relationship between two variables, these statistical methods have advantages over ML techniques. However, when this is not the case, ML models may be more advantageous and include many options to explore different types of relationships simultaneously. [54,55] ML models have been widely utilized in bioinformatics and biomedical sciences with the proliferation of big data because it allows the modeling of systems and risk factors with a greater level of complexity.[57,58]

The model fit can be evaluated using differences between the predicted and true classification, i.e., accuracy, precision. Model fit is influenced by model's robustness to noise (variance) and the inability to capture or simulate the situation it is addressing (bias). An overly complicated or overfitted model may demonstrate low bias and high variance such that it performs perfectly on a training dataset, i.e. the data used to create the model, but very poorly when using new data.[59–61] The model building process entails selection of inputs, creating testing and training datasets to avoid model overfitting, and ensuring that the model captures the clinical or physiological perspective so it is relevant.

A recent meta-analysis[53] evaluated fifty-five different machine learning prediction models used in cardiology, on the same data from one million patients. Included models were designed to represent coronary artery diseases, heart failure, arrhythmias, and stroke. Most of the studies were focused on risk assessment and the meta-analysis concluded that ML models have reliable accuracy and satisfactory area under the curve (AUC) results. However, they are not yet optimal for clinical practice as most show significant heterogeneity in the model building process or lack of transparency for the modeling building process.

Another notable observation for ML applications in cardiovascular medicine is that model selection is not well described and models are not validated.[53] It is possible that several models were developed and only the most accurate model was reported. This is particularly a concern when models are not validated. Validation helps to eliminate concern regarding overfitting and reproducibility. Therefore, it is recommended that the stages of model designing and interpretation should be clear, transparent and if possible, replicated on other studies or a validation dataset.[53,62]

To decipher our questions about the fibrotic remodeling pathways in a phenotype of postmenopausal women at older age with pressure overload in HFpEF, we chose an artificial neural network machine learning model. This model allows us to explore different types of relationships and to perform classification modeling.

Artificial Neural Networks

General structure: Artificial neural networks (ANN) are a type of machine learning model inspired by how the human brain processes information and have been applied for over four decades in cardiovascular field and other medical fields in general.[63–65] An artificial neural network works to mimic a biological neural network through an interconnected network formed of processing units called nodes or neurons. The neurons can be divided according to their roles (i.e. input, hidden and output neurons) and their communication is achieved through weighted connections, or functions, between the neurons in different layers, or groups of neurons. Input layer neurons are presented with "signals" or input data from different features. The input neurons of each feature use functions to add weights and bias terms to each and then that information is sent to the next layer of neurons. Layers which are not input or output layers are called hidden layers. The neurons in a hidden layer activate a transfer function, or activation function, and then sum the weighted, processed data to the next layer of neurons. This transfer occurs in a similar fashion to the signal processing within neurons and signal transfer through synapses. A neural network can have one or more hidden layers which add more processing units and add to the pattern recognition capacity of the neural network. Data is then transferred to the output layer neurons which activates a transfer function and sums all signals generating an output. Unlike their biological counterparts, ANNs calculate an

error and repeat the same process again. The calculated error is used to alter the weights in the next iteration until the neural network reaches the best set of interconnections or weights for each input data. This occurs when the error is minimized.[66–68]

Activation function: The transfer functions, or activation functions, can be selected and/ or tailored which allows the neural network to perform several types of tasks. For example, the logarithmic activation function can be used to explore linear relationships, while the hyperbolic tangent function can be used to explore non-linear relationships. For more complicated models, a combination of several activation functions can be used on different layers, but this must align with the purpose of the ANN model. [67,69]

Weights and the learning stage: The neurons in the network are assigned weights, as information moves from layer to layer. These weights are optimized with each iteration to obtain a correct output for each input. After calculating the output, error is defined as the difference between the output and the true data value from the training dataset.[66] After training is complete, the final values of weights associated with the data from each neuron, connecting input and output layers, are stored for the model trained using a given dataset.[67] The error calculation and iterative weighting process determines the learning ability of the model. In addition, changing the rate and the number of iterations performed by the ANN can influence a model's performance.

Model testing / performance evaluation: After training, the ANN model is evaluated using a testing dataset, a new set of data with the same input features as the training dataset. Using the testing data, the ANN model performance is considered satisfactory if the model's ability to analyze the data patterns during the training stage could be

generalized so as the model can predict an output from the testing dataset is in agreement with the actual output. [68]

Advantages and disadvantages of ANN: ANN are advantageous for problems that involve complex systems, with limited known information, and can detect possible interactions between input variables. In addition, ANNs are resistant to noise and can perform pattern recognition, abstraction, and generalization on both categorical and continuous variables.[69] In contrast to many other prediction techniques, ANNs do not inflict restrictions on the distribution for the input features, from different probability distributions, and data with non-constant variance. Utilizing different activation functions allows the ANN to perform both classification and prediction problems with similar efficacy.[70]

However, ANNs require greater computational resources than simpler statistical methods. With current computational capacities, this is no longer an obstacle. There is no specific rule for determining the structure of ANN, therefore model training and developing is empirical. Further, ANNs like other machine learning models, are prone to overfitting.[63,70,71]

Large animal models in HFpEF

Most of our current knowledge about the cellular and molecular mechanisms identified in cardiovascular medicine comes from small animal models, murine models in particular. However, a common limitation in expanding this knowledge to clinical application is the discrepancy between small animal models and humans, in terms of metabolism and oxygen consumption, heart rate, contractile protein abundance and the excitation contraction coupling, besides the evident heart and body size difference between species.[72] Small animal models provide many advantages relative to other animal models including the low cost and space requirements, availability, ease of generating transgenic models and short life span. This allows the modeling of diseases over the entire animal lifespan and increasing sample size conveniently.[72,73]

Large animal models provide a relatively closer approximation to human physiology, anatomy and multiple systems, neural and hormonal connections. On the other hand, the long lifespan of animals mandates a longer generation time for the model. In addition, fewer available transgenic models are available, while large animal models require more intense labor, specialized facilities and associated costs. All these issues limit large animal model utilization in basic and translational research. Nevertheless, the translational value and advantages provided by large animal models is necessary for modulation of many diseases, especially for diseases like HFpEF.[74]

Swine models have been popular in cardiovascular research. The heart size, immune response, physiology and anatomy of heart and coronaries resemble the humans to a greater extent relative to any other animal model. It is argued that the swine heart resembles a young human heart in terms of vascular anatomy and coronaries that do not

develop collateral circulation. Swine models used for surgical modeling of various cardiovascular conditions like ischemia and pressure overload, manifest variability between procedures in a better simulation to clinical setting. On the down side, swine models are associated with relatively higher rates of post-operative complications and the incidence of tachyarrhythmia and sudden death.[74]

Despite the urgency of gaining better understanding and developing effective treatment for HFpEF, the lack of translational animal models hinders research ability to comprehend the various systems contributions, coexisting comorbidities and predisposing factors associated with the disease. Therefore, development of preclinical models that include different phenotypes of HFpEF has been a challenge in order to advance the understanding of the heterogeneous, growing population of HFpEF patients.[75]

An ideal animal model for HFpEF should have the potential to recapitulate all the key phenotypes and comorbidities observed in HFpEF patients which could be an unrealistic goal for a single model. Large animal swine models can recapitulate human physiology, encompassing cardiac and non-cardiac contributors in HFpEF which is essential to elucidate the pathophysiology of the disease phenotypes, molecular mechanism and incorporate this knowledge into clinical interventions.[6,76] Therefore, a preclinical swine model for HFpEF was chosen to generate the dataset for fibrosis evaluation.

Conclusion

Understanding the fibrotic remodeling process on both ventricles is an important missing piece of the puzzle for linking hemodynamic changes between systemic and pulmonary circulation as a part of the overall pathogenesis of HFpEF. Developing tools for

elucidating cellular and molecular mechanisms responsible for accumulation of ECM is essential for designing cardioprotective and therapeutic strategies to prevent or regress fibrosis, a main factor in HFpEF pathogenesis.[77] In order to address this complex, pathological process with differing disease phenotypes, many predisposing factors, and the intertwined nature of the fibrotic remodeling process itself, computational modeling is a logical next step. These types of models allow integration of several results, can model molecular level data in tandem with organ level outcomes, and are not unique to specific translational models of disease. .[6,78,79] The model development must reflect the physiology as well as be meaningful for clinical application.

My study combines these two recommended approaches to address maladaptive fibrotic remodeling process in HFpEF (i.e. large animal models and computational machine learning analysis) as summarized in figure 1-1. Given significant sex disparities noted in HFpEF prevalence, a preclinical swine study was conducted to assess the role of female sex hormones on chamber-dependent differences i.e., left ventricle (LV) vs. right ventricle (RV), in cardiac fibrosis, using measurements of extracellular matrix (ECM) components. Specifically, a mini-swine Yucatan model of pressure overload-induced heart failure and menopause is used to model these conditions. Using data collected from this pre-clinical experiment, the aim of this study is to build an ANN model using a selected number of ECM variables to test their importance in the fibrotic remodeling pathways in the presence of pressure overload and loss of female sex hormones phenotypes of HFpEF. These results will elucidate these potential mechanisms through this pre-clinical swine model of HFpEF.

Chapter two: METHODS

Female Yucatan swine model of HFpEF and fibrotic remodeling assessment and dataset generation.

Experimental design: A pre-clinical mini-swine Yucatan model of HFpEF was used. HFpEF is induced through surgical interventions of aortic banding and ovariectomy to model aortic pressure overload and loss of female sex hormones, respectively. The experimental study was designed as a two factor, crossed study with two independent factors, aortic banding (AB) and ovariectomy (OVX). Animals that did not undergo aortic banding were defined as controls (CON) and animals that did not undergo ovariectomy were defined as intact (INT). Sexually mature, female swine at 7 months of age (N = 24) were assigned to four experimental groups: 1) control-intact (CON-INT) (n=6), 2) aortic-banded intact animals (AB-INT) (n=7), 3) control (non-aortic banded) ovariectomy (CON-OVX) (n=5), and 4) aortic-banded with ovariectomy (AB-OVX) (n=6). These are the same animals used in Olver et al [80].

Ovariectomy was performed at 7 months of age, one month before aortic-banding, to confirm the loss of endogenous sex hormones before initiation of the pressure overload intervention at 8 months of age. At 14 months of age, terminal surgeries were performed after 6 months of pressure overload. After euthanasia, tissue samples were obtained from both right and left ventricles. Measurements from qRT-PCR, Western blot, and zymography and fluorogenic substrate assay were used to generate all data. All experimental animal protocols used in this study were in accordance with Principles for the Utilization and Care of Vertebrate Animals for Testing Research and Training

approved by the University of Missouri (Columbia, MO) Animal Care and Use Committee.

Ovariectomy: Animals were sedated with Telazol (tiletamine hydrochloride and zolazepam hydrochloride)/xylazine (5.0/2.25 mg/kg) and maintained under anesthesia with 3.0% isoflurane. A midline incision was used to expose left and right ovaries. Ovaries were excised completely after arteriovenous complex ligation with 0 absorbable suture. After transection, the ovarian bursa was opened to inspect the ovaries and confirm complete ovarian removal. [81]

Aortic Banding: The aortic band was placed around the ascending aorta to achieve a systolic trans-stenotic gradient of approximately 70 mm Hg. The procedure was conducted under equivalent hemodynamic conditions for all pigs. Mean arterial pressure (MAP) under anesthesia was maintained at approximately 90 mm Hg using phenylephrine and heart rate was ≈100 beats per minute. There was no statistically significant difference in hemodynamic conditions between the four groups as reported previously in Olver et al[80]. Left ventricular brain natriuretic peptide mRNA was measured to assess heart failure as previously reported by our laboratory.[82,83]

Fibrotic remodeling dataset generation

qRT-PCR: Samples were flash frozen using liquid nitrogen and stored at -80°C until processed. Quantitative Real Time-PCR (qRT-PCR) of total homogenate from RV and LV was performed using the 2-ΔΔCt method as previously described.[84,85] Targets included mRNA levels of estrogen (isoforms 1, 2) , progesterone receptors and progesterone receptor membrane component 1; ERK/JNK pathway signaling and

regulation including MAPK isoforms 1, 3, 8, and 9, MAPKK isoforms 1, 2, 4, and 7, and dual specificity phosphatases (DUSP) isoforms 1, 4, 6, 9, and 10; matrix metalloproteinase (MMP) isoforms 1, 2, 3, 9, 13, and 14; tissue inhibitors of MMP (TIMP) isoforms 1, 2, and 4; the ECM components collagen (isoforms 1 and 3) and fibronectin. All quantified targets can be found in table S-1.

Western Blot: Proteins from RV and LV homogenized samples were extracted using sonication in Laemmli buffer (62.5 mM Tris, pH 6.8, 6 M urea, 160 mM dithiothreitol, 2% SDS, and 0.0001% bromophenol blue). NanoOrange assay (ThermoFisher) was used to determine protein concentration to be used. Proteins were run in SDS loading buffer on 4-20% SDS/PAGE acrylamide gels before transfer to PVDF membranes. Membranes were blocked in 2.5% non-fat milk, then incubated at 4°C in primary antibodies overnight. Horseradish peroxidase-linked secondary antibodies were applied to the membrane prior to imaging using Luminata Forte Western Chemiluminescent HRP substrate reagent (EMD Millipore). For normalization of detected protein levels, the loading control utilized was Coomassie blue. The detailed western blots process was previously described in detail.[49,86] Quantified protein levels included protein levels of Estrogen receptor alpha and beta isoform , Progesterone receptor isoform(A,B) , Progesterone receptor membrane component ERK/JNK (total and phosphorylated), MMP14, TIMP2, and fibronectin.

Zymography: Gelatin zymography was used to analyze activity and abundance of MMP isoforms 2 and 9. Protein concentration in the homogenized RV and LV tissue samples was determined using BCA protein assay. 100µg total protein was prepared in 4x sample buffer (250 mM Tris-HCl, pH 6.8, 40% v/v glycerol, 8% SDS w/v, 0.01% w/v

bromophenol blue). Total proteins of each sample were run on 10% zymography gel (Invitrogen) for 110 minutes at 125 V which were incubated in zymography renaturing buffer (Invitrogen) for 30 minutes at room temperature with slight agitation. This was followed by incubation in zymography developing buffer and staining with Coomassie blue (0.5% w/v Coomassie, 5% v/v methanol, and 10% v/v acetic acid in H2O) for one hour followed by destaining using buffer (10% v/v methanol and 5% v/v acetic acid in H2O) to obtain the optimum resolution of bands. Gel imaging was performed using Azure Biosystems c600 Imager and quantified with ImageJ software.[49,87]

Statistical analysis: Statistical analysis was conducted using RStudio version 4.0.3 and GraphPad Prism 9.2.0. Two-way ANOVAs were used to identify main effects or interaction between the experimental interventions (OVX and AB) on each measurement. Uncorrected, Fisher's least significant difference was used for post hoc analysis. All data is presented as mean ± SEM. Significance level is reported at the $P < 0.10$ and $P < 0.05$ levels.

Artificial neural network building and performance evaluation

Data preprocessing: In general, missing data can have a negative impact on the statistical power of the study and produce biased estimates, leading to invalid or unreliable conclusions.[88] The R software default in most functions is case-wise deletion, which introduces loss of power, decreases sample size, and increases potential bias.[89] Specific to this study, artificial neural networks are not able to accommodate missing data. Therefore, we must impute missing values prior to model development for the ANN.[90,91]

Mean imputation is one of the most widely used imputation methods, although it is only recommended when there is a small proportion of missing data to replace[92], as observed here. Mean imputation is the process of replacing missing data with estimated mean values. In this approach, the mean value for all of the non-missing values of a measurement is calculated and then this value is substituted for all missing values for that variable. [92]

The main concerns for using mean imputation are the underestimation of variance between measurements and the smaller standard errors. These smaller errors are due to the increased sample size from imputation which may not adequately reflect the uncertainty.[92,93] As a deterministic imputation method, it offers the advantage of more efficient estimates than imputation methods which use random selection, as the variability introduced by random selection is avoided.[94] In this study, these drawbacks were addressed by using within-group mean imputation. This method replaces the missing value with the mean for each homogenous group, here defined by the experimental group status .[95] This method, which lessens the reduction of variance, is a reasonable imputation method due to the relatively low amount of missing data and the physiological nature of the dataset.

Three subjects had a significant amount of missing data (~ 46 %) from LV measurements, due to limited tissue availability, therefore, these three subjects were excluded from further analysis. The remaining dataset was composed of 2,304 separate measurements from 24 subjects and the few remaining missing data points (0.0013 % of the total data points) were mean imputed using within-group mean imputation.

After imputation, a complete data set for the 24 subjects was obtained. From these 2,304 non-missing measurements, large differences in units or scales considered across measurements was observed. Because ANNs are sensitive to these differences, one must account for these differences in scale. One universally recommended method is to normalize the dataset. The normalization process can be implemented in different ways but among the most frequently applied approaches is the min–max normalization method. This method separately re-scales each measurement from the data by subtracting the minimum value of the measurement and dividing the difference by the range of that measurement (Eq. 1).[96]

$$x' = ((x - Xmin)/\,(Xmax - Xmin)), \qquad \textbf{Eq.(1)}$$

where, *x* is the attribute value to be normalized, *Xmax* is the maximum value of attribute *x*, and *Xmin* is the minimum value of attribute *x*.

More broadly, min-max normalization is a linear transformation of each measurement, mapping each value to the [0,1] domain. The main advantage of min-max normalization is that it preserves the monotonic relationships among the original data values. [97] Data assessment, imputation, and normalization was conducted using RStudio version 4.0.3 using packages "ggplot2" and "tidyverse".

Feature selection: The goal of this study is to build a classification model for the experimental group status, such that results would provide useful insight for human cardiac clinical care. As the clinical presentation for HFpEF is multifactorial, it was important to structure the ANN such that it reflects the likely unknown disease status. To build an ANN which reflects this, we must first select the input features to be included. This selection should be influenced by the nature and goals of the original research question being assessed and consider the biological meaning and clinical relevance. For

example, if we design a model that needs 50 input variables for satisfactory performance, the burden and cost of obtaining that information will limit the utilization and translational potential of the model, even if we maximize the overall accuracy. Therefore, feature selection, or model input, is of utmost importance.

One method to identify features for inclusion is to identify those which show significant variation among the important outcomes, here experimental group status. One way ANOVA was used to determine mean differences for each measurement by experimental group status. These differences serve as an indication for physiological change and contribution to the remodeling process following these interventions of aortic banding and/or ovariectomy. The chosen cutoff for statistical significance was set at a two-sided p-value of 0.1, to be more inclusive with potential features of interest. Measurements identified as different using these one-way ANOVAs were used as input features for the ANN.

Among the many machine learning models, neural network models are attractive for diagnostic tasks, because of the challenging interconnected, complex nature of physiological data for classification problems. ANNs can be represented as a set of connected networks between inputs and outputs in which each connection is associated using an assigned weight. ANNs consists of one input layer, one or more intermediate layers called the hidden layers (where most calculations take place), and one output layer. The learning process of a neural network is performed by adjusting the weight for connections in an iterative process, to improve overall performance. One such learning method, backpropagation, is a gradient descent (partial derivative) based method for error minimization. Backpropagation is the most commonly used and the simplest feedforward

algorithm, or algorithm with one direction of information flow, used for classification. [98–101]

Model optimization

The dataset was randomly partitioned such that at least one subject from each experimental group is included in the testing dataset (at least 4 subjects out of 24) while the rest of the subjects (at least 18) were used in the training dataset. The training data is used to create the ANN while the testing data would be used for model validation. Four-fold cross validation was used to induce variation in both testing and training datasets and each fold resulted in a complete ANN with a defined accuracy. Across the folds, the accuracy was averaged to calculate the overall accuracy of the ANN (figure 2-1).

Splitting the dataset into different folds of

To optimize the ANN, model fitting and accuracy criteria had to be determined; for this model, the overall model's accuracy and simplicity, for reproducibility purposes, prioritized accuracy scores (F1 score, percent accuracy, and balanced accuracy). For this ANN, a confusion matrix was used to determine the model's accuracy.

ANN model development included calculating model accuracy, optimizing the model's number of hidden layers, separately, optimizing the number of nodes in each layer, considering different activation functions, and different rates of learning. The number of layers considered ranged from one to two layers in order to adhere to machine learning approach and not deep learning, the number of nodes for each layer ranges from eight to two. Activation functions considered included the linear logistic, nonlinear Tanh, and a combination of the nonlinear Relu on the hidden layers and Softmax for the output layers.

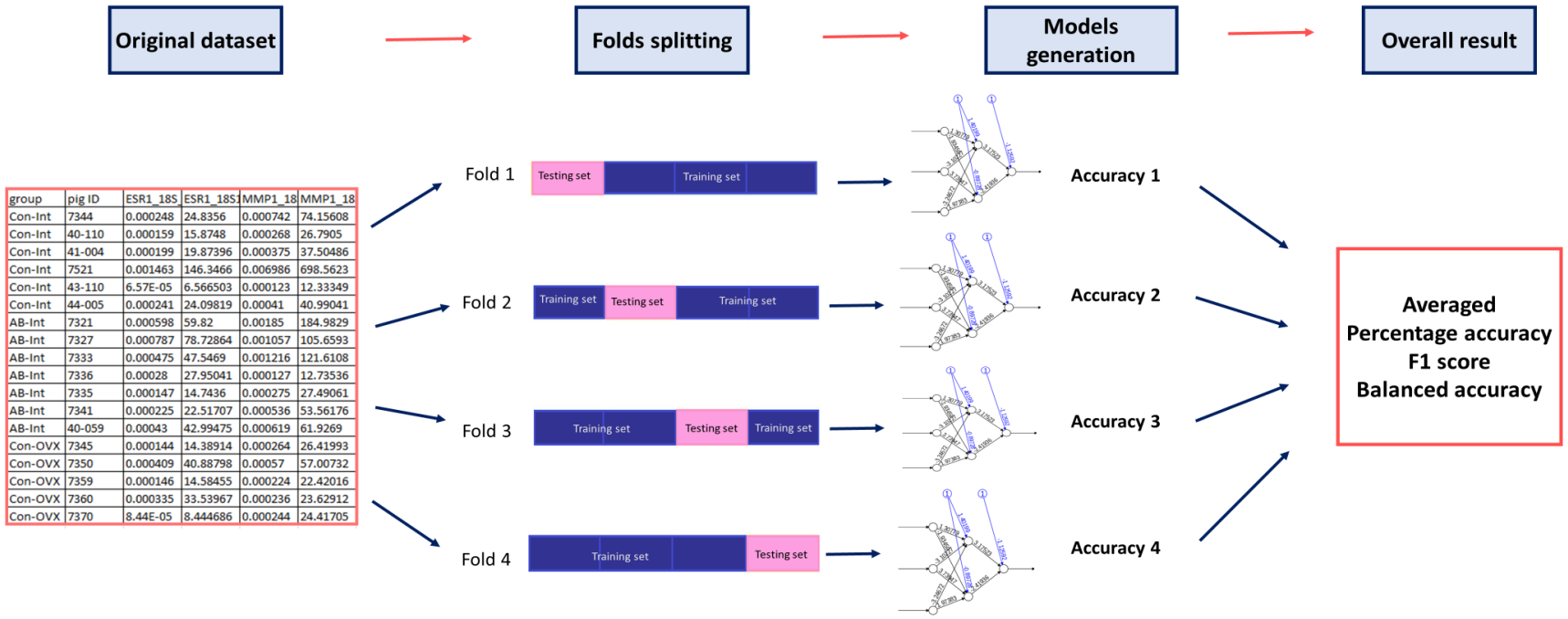

group	pig ID	ESR1_18S	ESR1_18S1	MMP1_18	MMP1_18
Con-Int	7344	0.000248	24.8356	0.000742	74.15608
Con-Int	40-110	0.000159	15.8748	0.000268	26.7905
Con-Int	41-004	0.000199	19.87396	0.000375	37.50486
Con-Int	7521	0.001463	146.3466	0.006986	698.5623
Con-Int	43-110	6.57E-05	6.566503	0.000123	12.33349
Con-Int	44-005	0.000241	24.09819	0.00041	40.99041
AB-Int	7321	0.000598	59.82	0.00185	184.9829
AB-Int	7327	0.000787	78.72864	0.001057	105.6593
AB-Int	7333	0.000475	47.5469	0.001216	121.6108
AB-Int	7336	0.00028	27.95041	0.000127	12.73536
AB-Int	7335	0.000147	14.7436	0.000275	27.49061
AB-Int	7341	0.000225	22.51707	0.000536	53.56176
AB-Int	40-059	0.00043	42.99475	0.000619	61.9269
Con-OVX	7345	0.000144	14.38914	0.000264	26.41993
Con-OVX	7350	0.000409	40.88798	0.00057	57.00732
Con-OVX	7359	0.000146	14.58455	0.000224	22.42016
Con-OVX	7360	0.000335	33.53967	0.000236	23.62912
Con-OVX	7370	8.44E-05	8.444686	0.000244	24.41705

Figure 2-1: An illustration of four-fold cross validation and accuracy calculations.

A confusion matrix (figure 2-2) contains all the predictions made by a model labeled according to the actual (true) classification they fall under in the original data and their predicted classification made by the ANN model. [102] Figure 2-2 presents the basic form of a confusion matrix for a multi-class classification task, with the classes A, B, and C and where V is the predicted value for each combination of classes. To calculate accuracy, these combinations must be coded to give a score which reflects the number of the "correct" predictions as a ratio of the total number of predictions. Based on this information, we can obtain the percent accuracy, sensitivity, specificity, precision, recall, F1 score, and prediction accuracy by experimental group. Among all these scores, the selection of the most appropriate accuracy measurement or score depends upon the broader goals for the model. For this research, we selected three accuracy scores to compare the performance of the model: percent accuracy, balanced accuracy, and F1 score. These scores provide an understanding for the model ability to classify the input values into the experimental group status collectively and the in each individual group. Percent accuracy is the number of correctly classified subjects divided by the total number of predictions. It provides an easy to perceive numerical value to describe the model performance, although it can misleading if not considered in context, especially with a small testing dataset like ours. Percent accuracy does not consider class imbalances, or the differing "costs" of false negatives and false positives; these are all considered equivalent. For example, if the ANN can predict the classes of 4 out of 4 subjects it will have a 100% accuracy and if another classifier predicts the classes of 30 out of 40 subjects it will have an accuracy of 75%. To address this, balanced accuracy for each experimental group was also considered to provide insight on differences in

predictions accuracy for classes. For example, a model used to predict classification of two groups A and B might be able to predict group A with an accuracy of 100% while group B is predicted with 0% accuracy.

F1 score can be defined as the harmonic mean of precision and recall for a model.

Precision is a measure of the accuracy for a specific class that has been predicted (Eq 2).

$$\boldsymbol{Precision} = \frac{\boldsymbol{TP}}{\boldsymbol{TP+FP}} \qquad \textbf{Eq.(2)}$$

where TP denotes the number true positives and FP denotes the number of false negatives

In a more direct definition, precision is the percentage of true positive predictions for all positive predictions. Recall measures the ability of the model to select retrieved instances among all relevant instances, i.e. sensitivity. Recall can be defined simply as the percentage of the actual positive predictions that were classified correctly. [103]

$$\boldsymbol{Recall} = \frac{\mathbf{TP}}{\mathbf{TP+FN}} \qquad \textbf{Eq. (3)}$$

where TP denotes the number of true positives and TN denotes the number of true negatives

Balancing both precision and recall, the F1 score provides a more nuanced accuracy score.

Feature selection and model building was performed using RStudio version 4.0.3 with package “neuralnet” for neural network algorithm and “caret” for confusion matrix and cross fold validation. One way ANOVA was conducted using GraphPad prism 9.2.0.

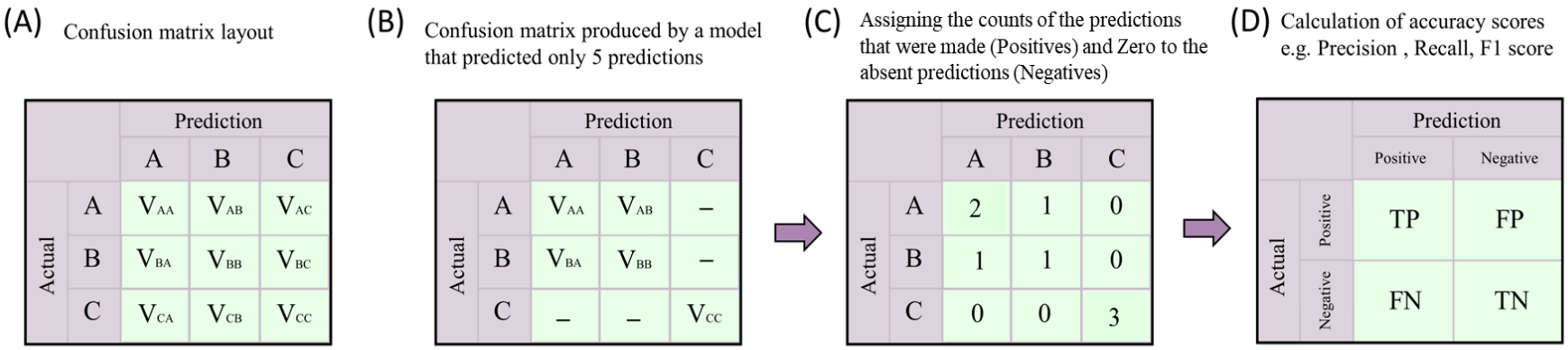

Figure 2-2: An illustration of accuracy calculation from a classification model using a confusion matrix. A) illustrates the typical structure of a confusion matrix where A,B and C denote the groups / classes predicted by the model and V is the predicted classes by the model. Only the outputs with matching actual and prediction classes are predicted correctly, B) is showing a confusion matrix produced by a classification model where some of the possible combinations between actual/predicted classes were not predicted, C) illustrates a simplification step where the number of predictions are made for each combination are listed, assigning count to the predicted combinations and a zero to the combinations that was not predicted by the model. D) Using the true and false positive and negative predictions to calculate the accuracy scores. Acronyms: TP; True positive, FP; False positive, FN; False negative, TN; True negative.

Chapter Three: RESULTS

Feature selection using one-way ANOVA identified nine ECM measurements that showed statistically significant differences between experimental group status (p-value < 0.1). The identified features were measurements from both the RV and LV and represent different steps of the fibrotic remodeling pathway. Table 1 and figure 3-1 displays the nine identified features and their level of significance. Since the number of input features identified was not relatively large, all were used as input features in the designed ANN model.

One way ANOVA results **statistical significance for variability among experimental groups**		
Variable	**Chamber**	**p-value**
Total collagen content	Left ventricle	0.016
Collagen I mRNA level	Left ventricle	0.094
MMP14 activity and/or abundance	Left ventricle	0.072
MMP2 activity and/or abundance	Left ventricle	0.086
TIMP1 mRNA level	Left ventricle	0.042
Total JNK protein	Left ventricle	0.070
Total collagen content	Right ventricle	0.017
Collagen I mRNA level	Right ventricle	0.092
Collagen III mRNA level	Right ventricle	0.064

Table 1: One Way ANOVA results of 9 measurements identified from 96 total ECM inputs that show statistically significant differences between experimental group status. Acronyms: MMP; Matrix metalloprotease, TIMP; Tissue inhibitor of matrix metalloprotease, JNK; c-Jun Amino-Terminal Kinases

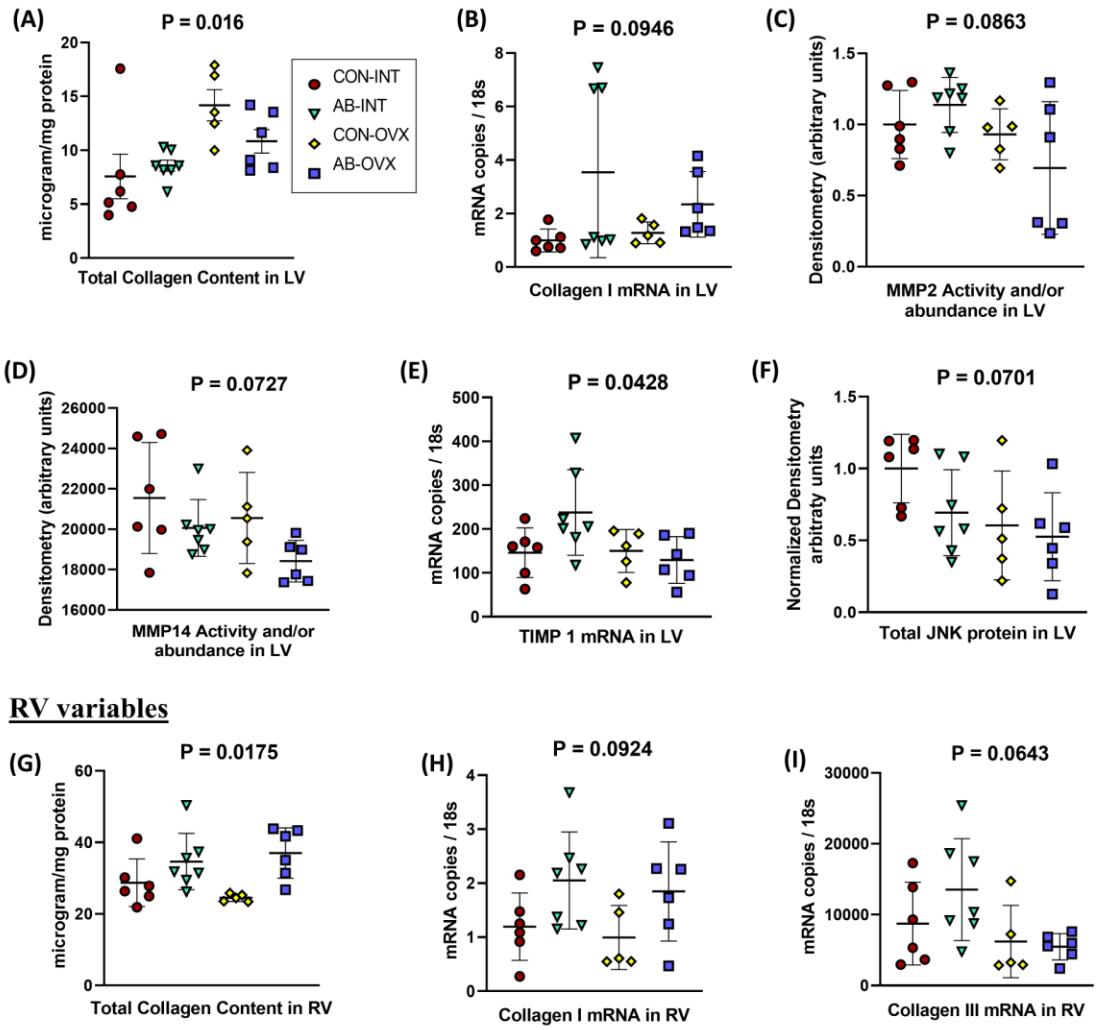

Figure 3-1: One Way ANOVA results showing nine extracellular matrix components with statistically significant mean differences between experimental group status (p-value < 0.1). Figures A-F show the components identified in the left ventricle and G-I show the right ventricle components. Acronyms: CON-INT; Control-intact, AB-INT; Aortic banded-Intact, CON-OVX; Control-ovariectomized, AB-OVX; Aortic bended-ovariectomized, MMP2; Matrix metalloprotease 2, MMP14, Matrix metalloprotease 14, TIMP 1; Tissue inhibitor of matrix metalloprotease 1, JNK; c-Jun Amino-Terminal Kinases, LV; Left ventricle, RV; Right ventricle.

The ANN model with the highest accuracy scores contained two hidden layers with eight and five nodes in the first and the second layers, respectively, and used the logistic activation function. The corresponding accuracy was 70.7% with F1 score of 0.81. The model features and results are shown in Figure 3-2.

To better understand potential physiological mechanisms, two-way ANOVA model results, with aortic-banding and ovariectomy as factors, were revisited from the original experiment but revised to only include data from the 24 subjects considered in the ANN. The results from these two-way ANOVAs confirm the discrepancy in the response of the individual variables between the two ventricles and the pathological conditions of pressure overload and loss of female sex hormones. As shown in Table 2 and Figure 3-3, loss of female sex hormones through ovariectomy was the main effect that led to a significant increase in the levels of total collagen content, and a decrease in levels of total JNK protein and MMP2 activity and/or abundance independently from pressure overload status in the LV. Pressure overload led to an increase in Collagen I mRNA level and a decrease in MMP 14 activity and/or abundance in the LV independently from loss of female sex hormone status. In the RV, ovariectomy significantly decreased collagen III mRNA levels. A main effect of pressure overload induced through aortic-banding led to an increase in total collagen content along with collagen I mRNA level in the RV. Changes in TIMP-1 mRNA levels resulting from pressure overload were dependent on female sex hormone status (interaction), with an increase observed in AB-INT animals.

Input features
Identified by One way ANOVA

Linear logistic activation function
2 Hidden layers With 8 and 5 nodes

Output
Experimental groups status

ANN algorithm
Back propagation and optimizing loss function

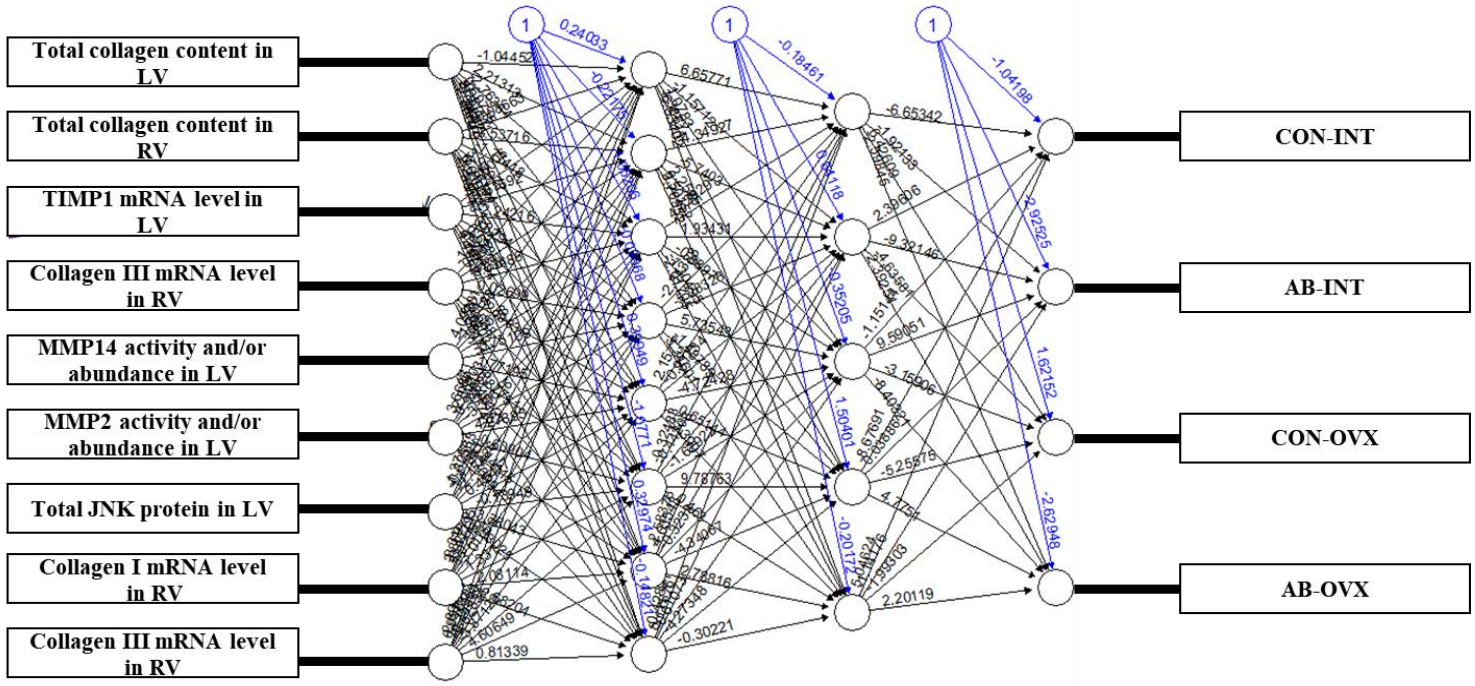

Accuracy (After cross validation and confusion matrices) :

F1 score 0.81 **Percentage accuracy 70.08 %** **Balanced accuracy : CON-INT : 71%**
AB-INT : 73%
CON-OVX : 93%
AB-OVX : 91%

Figure 3-2: Artificial neural network with the most optimum outcomes for prediction of experimental group status based on 9 ECM identified variables. The nine identified input features included ECM components from different levels of the regulatory cascades including ECM fibrous proteins, Matrix metalloproteases and their tissue inhibitors and upstream kinases like c-Jun Amino-Terminal Kinases. The model predicted the experimental group status with an accuracy of 70%, 0.81 F1 score and balanced accuracy for each group was 71% for control-intact, 73% in aortic banded-intact, 93% in control-ovariectomized animals and 91% in aortic banded-ovariectomized animals. Figures A-F show the variables identified in the left ventricle and G-I show the Right ventricle variables.

Acronyms: CON-INT; Control-intact, AB-INT; Aortic banded-Intact, CON-OVX; Control-ovariectomized, AB-OVX; Aortic bended-ovariectomized, MMP2; Matrix metalloprotease 2, MMP14, Matrix metalloprotease 14, TIMP 1; Tissue inhibitor of matrix metalloprotease 1, JNK; c-Jun Amino-Terminal Kinases, LV; Left ventricle, RV; Right ventricle.

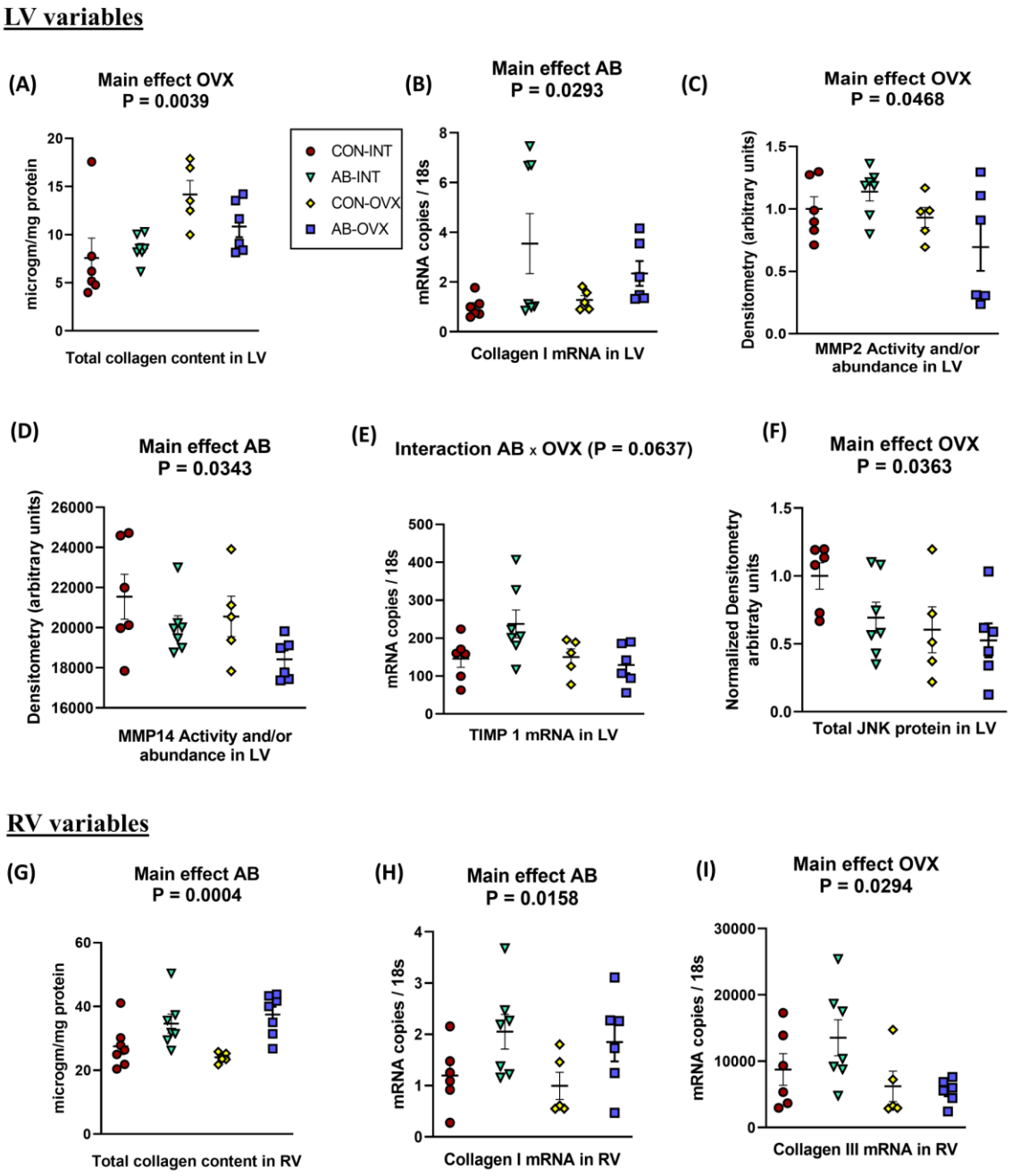

Figure 3-3: Two-way ANOVA results for the 9 ANN features, followed by uncorrected Fisher's least significant difference post-hoc test, where significant p-values are < 0.05. Figures A-F show the variables identified in the left ventricle and G-I show the right ventricle variables. A) Ovariectomy increases total collagen content in the LV regardless of aortic banding status. B) A

main effect of aortic banding induced pressure overload that increases mRNA levels of collagen I in the LV independently from ovariectomy. C and F) Ovariectomy decreased the activity and/or abundance level of MMP2 and JNK levels in the left ventricle regardless of aortic banding status in the LV. D) Aortic banding reduced MMP14 activity and/or abundance level in the LV independently from Ovariectomy effect. E) Change in TIMP1 mRNA levels by aortic banding was dependent on ovariectomy status. G) and H) Main effect of aortic banding that increases total collagen content and mRNA levels in the RV regardless of ovariectomy status. I) Ovariectomy increases collagen III mRNA level in the RV regardless of aortic banding status.
Acronyms: CON-INT; Control-intact, AB-INT; Aortic banded-Intact, CON-OVX; Control-ovariectomized, AB-OVX; Aortic bended-ovariectomized, MMP2; Matrix metalloprotease 2, MMP14, Matrix metalloprotease 14, TIMP 1; Tissue inhibitor of matrix metalloprotease 1, JNK; c-Jun Amino-Terminal Kinases, LV; Left ventricle, RV; Right ventricle.

Type of Effect	Chamber	
	LV	**RV**
OVX **Main effect P<0.05**	**↑ Total collagen content** **↓ total JNK protein level** **↓ MMP2 activity**	**↓ mRNA level of Collagen III**
AB **Main effect P<0.05**	**↓ MMP14 activity** **↑ mRNA level of Collagen I**	**↑ in Total collagen content** **↑ mRNA level of Collagen I**
OVX and AB Interaction **P = 0.06**	**The Δ in TIMP1 mRNA level is dependent on the ovariectomy status**	

Table 2: Interpretation of two way ANOVA results in each ventricle based on the main effect of each independent variable i.e., aortic banding (AB) or ovariectomy (OVX) or an interaction between the two variables (ABxOVX).

Acronyms: CON-INT; Control-intact, AB-INT; Aortic banded-Intact, CON-OVX; Control-ovariectomized, AB-OVX; Aortic bended-ovariectomized, MMP2; Matrix metalloprotease 2, MMP14, Matrix metalloprotease 14, TIMP 1; Tissue inhibitor of matrix metalloprotease 1, JNK; c-Jun Amino-Terminal Kinases, LV; Left ventricle, RV; Right ventricle.

Chapter Four: DISCUSSION

The aim of the developed ANN was to predict experimental group status, i.e., pressure overload and loss of female sex hormones, using features measured from the ECM. One way ANOVA results identify key ECM components including structural proteins, regulatory enzymes, and cellular signaling pathways that may be associated with pressure overload and loss of female sex hormones in a preclinical model of HFpEF. The results obtained from ANN using these ECM components as predictors provide new insight on the importance of these variables in the ECM remodeling pathways. Furthermore, these results reinforce that chamber-specific differences play a role in the pathological fibrotic remodeling process.

Using a statistical method with higher resolution and power is one approach for identifying the input variables, yet choosing one method or the other depends on the objectives of the model. The overall purpose of this ANN model is to find a number of biventricular variables in the fibrotic remodeling pathway that can be used as a start for future investigation to get a better understanding about the pathogenesis. While the study design followed a two by two cross design, using two way ANOVA on each variable in the dataset indicated that many ECM variables show a main effect of one of the independent variables (ovariectomy or aortic banding), or an interaction between the effects of the two interventions which identify a large number of variables. Using one way ANOVA which has less resolution require a larger difference in the mean between groups in order to have a statistically significant difference and therefore allows us to identify a more limited number of variables to satisfy the reproducibility and future

validation of the model. The utilization of more input variables limits the reproducibility of the model in future studies and clinical practice, and most importantly, doesn't guarantee better model accuracy. On the contrary, it limits our ability to detect the most important features.

The reported ANN with the best performance used a linear logistic activation function which aligns with the linear nature of the feature selection process used, i.e. one way ANOVA method. Nine features included in the ANN were from mRNA levels of collagen I and III, the quantified total collagen proteins in both ventricles, regulatory enzymes like MMP-2 and -14 and TIMP-1, and upstream kinases like total JNK. Without further computational work, the ANN model does not give clear understanding of feature importance. To address these points, the two way ANOVA was conducted for the included data to give a clearer insight into magnitude and directionality of association for each feature and the experimental group status.

As summarized in Table 2, pressure overload was the main effect for total collagen content accumulation on the RV while in the LV, it was loss of female sex hormones. The exact reason behind this difference in response is still unknown, although our limited dataset shows a significant difference in sex hormone receptor levels between the two ventricles in normal healthy animals. i.e. the control-intact group. Using paired student t-test, the left ventricle showed a higher levels of female sex hormone receptors mRNA than the right ventricle. Specifically, estrogen receptor (ESR-1) mRNA levels ($P = 0.041$) and ESR2 mRNA ($P = 0.0148$) were greater in the LV. There were no differences in progesterone receptors mRNA levels between the two ventricles. In addition, two way ANOVA results on ESR1 receptors mRNA in the LV show an increase in their levels as a

result for a main effect of pressure overload independent from loss of female sex hormones condition (P = 0.042). ESR1 mRNA in the RV and ESR 2 in both RV and LV show no significance difference between groups. Despite these findings, none of the sex hormone receptors or membrane components showed a significance difference between the experimental groups when evaluated using the one way ANOVA and therefore, were not included in the model. This illustrates why feature selection process is essential for the model building and why we chose narrowing down the input features using one way ANOVA and how the biological value of an input variable alone in no indication for how it will affect the machine learning model's performance unlike what's expected in the statistical approaches.

Estrogen plays a role in many remodeling pathways in the cardiac tissues including hypertrophic signaling, ROS production, density and expression of calcium channels in addition to extracellular matrix[104–106]. Estrogen receptor density correlation to the function of each ventricle needs investigation in the setting of healthy conditions versus pathological remodeling and could provide further understanding about the left and right ventricles fibrotic pathological remodeling in a postmenopausal phenotype of HFpEF. Progesterone receptors also play a protective cardiovascular role. Progesterone receptors pathways play a role in regulation of blood pressure inducing vasodilation, have a protective effect against cardiac fibroblast activation, regulates contractile properties and oxidative metabolism in the heart although it is not as extensively studied compared to estrogen effect.[107–109] While sex hormone receptors were not included as predictors in our ANN model, the results do not deny the overt role they play through the loss of female sex hormones in HFpEF especially given the model had higher accuracy in prediction of

ovariectomy groups (93% and 91% for control-ovariectomy and aortic banding-ovariectomy groups respectively).

The mRNA levels of both quantified collagen subtypes also showed a different response to our two experimental interventions. Collagen I represents approximately 80% of total collagen content and is associated with more stiffness while collagen III constitutes approximately 11% and is more predominantly responsible for elasticity of cardiac ECM.[46,110] In our pre-clinical model, collagen III subtype mRNA levels decreased in the RV due to loss of female sex hormones while Collagen I mRNA levels in both LV and RV increased with AB. The translation of these results into a change in the ratio of collagen I/collagen III protein levels in still under investigation.

The remaining features represent regulatory pathways for ECM remodeling and arguably have important value from a clinical perspective, due to the accessibility and availability for these measures which uses a non-invasive method of data collection. Our results agree with the findings of a recent meta-analysis[46] conducted on 23 animal studies focused on left ventricular diastolic dysfunction and HFpEF. Results indicated it is unlikely that an individual MMP or TIMP levels or activity would have a sufficient predictive value and that the activity of these regulatory enzymes have a more established predictive role over their quantified circulating levels. This supports the overall clinical purpose of our model as we show that MMP 2 and 14 activity and/or abundance were among the identified predictors. The difference shown in the changes and directionality between MMPs and TIMPs levels and activities in our results also support that using ECM regulatory enzymes as predictors or biomarkers for fibrotic remodeling cannot depend on a single variable and it needs to be addressed in a chamber dependent manner.

One limitation for this ANN model is that non-linear relationships between other measurements and the experimental group status could exist. Another limitation is the cross-sectional nature of the data, as all measurement were collected after euthanasia, which was six months after induction of pressure overload. This limits the understanding of the sequential process of the ECM fibrotic remodeling in each of the experimental groups. Investigating potential non-linear relationships for feature selection will be addressed in future work to identify mechanisms in the ECM remodeling pathway in HFpEF phenotypes, using pre-clinical models of pressure overload and loss of female sex hormones. Future work will also consider improving the overall model's predictive accuracy. Investigating the interrelationships between these nine predictors will provide a long needed understanding of the fibrotic remodeling pathogenesis on both sides of the heart in HFpEF which can be used to identify biomarkers or therapeutic targets tailored according to the present phenotype.

Noninvasive biomarkers for fibrotic remodeling have been investigated as prognostic markers in HFpEF and have shown predictive value over standardized markers for myocardial stretch and stress like BNP and NT-proBNP.[111–113] In a clinical setting, quantifying some of the identified ECM regulatory components used in our model (e.g MMP2, MMP14 and TIMP1) in patients presented with hypertension, post-menopausal women and/or belong to an older age group can be used as an indication for the activation of fibrotic remodeling pathway and myocardial stiffness and therefore as a risk assessment for HFpEF. In a cross sectional study on hypertensive patients MMP2 was proposed as a predictive marker for HFpEF with equal or better sensitivity and specificity to BNP.[111] In previous clinical study on plasma biomarkers for fibrotic remodeling

associated with exacerbation of HFpEF symptoms, It was concluded that MMP2 plasma levels is an independent marker for extracellular volume that's significantly associated with global interstitial fibrotic remodeling. TIMP1 in the same study showed higher levels in HFpEF patients with myocardial fibrosis assessed through cardiac magnetic resonance imaging.[114] TIMP1 was also a significant predictor for diastolic dysfunction in HFpEF in another clinical study on patients with atrial fibrillation.[115]

In addition, right ventricle predictors can have a higher importance in particular phenotypes of HFpEF with pulmonary hypertension and right side heart failure.

Overall, this ANN model using data from a preclinical animal model identified nine important ECM components that can be used as a start in future research to understand the fibrotic remodeling pathway in HFpEF pathogenesis. The results also indicate the importance of addressing right and left ventricles remodeling differences especially for a disease like HFpEF where hemodynamic linkage between the two sides of the heart could play an essential role in the manifestation of disease phenotypes.

References

1. Oktay AA, Rich JD, Shah SJ. The Emerging Epidemic of Heart Failure with Preserved Ejection Fraction. *Curr Heart Fail Rep*. 2013;10:10.1007/s11897-013-0155–7.

2. Roger VL. Heart Failure Epidemic. *Circulation*. 2018;138:25–28.

3. Ba B. The pathophysiology of heart failure with preserved ejection fraction. *Nature reviews Cardiology*. 2014;11. doi:10.1038/nrcardio.2014.83.

4. Simmonds SJ, Cuijpers I, Heymans S, Jones EAV. Cellular and Molecular Differences between HFpEF and HFrEF: A Step Ahead in an Improved Pathological Understanding. *Cells*. 2020;9:242.

5. Oktay AA, Rich JD, Shah SJ. The Emerging Epidemic of Heart Failure with Preserved Ejection Fraction. *Curr Heart Fail Rep*. 2013;10:10.1007/s11897-013-0155–7.

6. Shah SJ, Borlaug BA, Kitzman DW, McCulloch AD, Blaxall BC, Agarwal R, Chirinos JA, Collins S, Deo RC, Gladwin MT, Granzier H, Hummel SL, Kass DA, Redfield MM, Sam F, Wang TJ, Desvigne-Nickens P, Adhikari BB. Research Priorities for Heart Failure With Preserved Ejection Fraction: National Heart, Lung, and Blood Institute Working Group Summary. *Circulation*. 2020;141:1001–1026.

7. Nair N. Epidemiology and pathogenesis of heart failure with preserved ejection fraction. *Rev Cardiovasc Med*. 2020;21:531–540.

8. Peeters JMPWU, Sanders-van Wijk S, Bektas S, Knackstedt C, Rickenbacher P, Nietlispach F, Handschin R, Maeder MT, Muzzarelli SF, Pfisterer ME, Brunner-La Rocca HP. Biomarkers in outpatient heart failure management; Are they correlated to and do they influence clinical judgment? *Neth Heart J*. 2014;22:115–121.

9. Shah SJ, Kitzman DW, Borlaug BA, van Heerebeek L, Zile MR, Kass DA, Paulus WJ. Phenotype-Specific Treatment of Heart Failure With Preserved Ejection Fraction: A Multiorgan Roadmap. *Circulation*. 2016;134:73–90.

10. Kalogeropoulos A, Georgiopoulou V, Psaty BM, Rodondi N, Smith AL, Harrison DG, Liu Y, Hoffmann U, Bauer DC, Newman AB, Kritchevsky SB, Harris TB, Butler J, Health ABC Study Investigators. Inflammatory markers and incident heart failure risk in older adults: the Health ABC (Health, Aging, and Body Composition) study. *J Am Coll Cardiol*. 2010;55:2129–2137.

11. DuBrock HM, AbouEzzeddine OF, Redfield MM. High-sensitivity C-reactive protein in heart failure with preserved ejection fraction. *PLoS One*. 2018;13:e0201836.

12. Mesquita T, Lin Y-N, Ibrahim A. Chronic low-grade inflammation in heart failure with preserved ejection fraction. *Aging Cell*. 2021;20:e13453.

13. Borlaug BA. The pathophysiology of heart failure with preserved ejection fraction. *Nat Rev Cardiol*. 2014;11:507–515.

14. Tanase DM, Radu S, Al Shurbaji S, Baroi GL, Florida Costea C, Turliuc MD, Ouatu A, Floria M. Natriuretic Peptides in Heart Failure with Preserved Left Ventricular Ejection Fraction: From Molecular Evidences to Clinical Implications. *Int J Mol Sci*. 2019;20:2629.

15. von Bibra H, St John Sutton M. Diastolic dysfunction in diabetes and the metabolic syndrome: promising potential for diagnosis and prognosis. *Diabetologia*. 2010;53:1033–1045.

16. Brouwers FP, de Boer RA, van der Harst P, Voors AA, Gansevoort RT, Bakker SJ, Hillege HL, van Veldhuisen DJ, van Gilst WH. Incidence and epidemiology of new onset heart failure with preserved vs. reduced ejection fraction in a community-based cohort: 11-year follow-up of PREVEND. *Eur Heart J*. 2013;34:1424–1431.

17. Pandey A, Omar W, Ayers C, LaMonte M, Klein L, Allen N, Kuller LH, Greenland P, Eaton C, Gottdiener JS, Lloyd-Jones D, Berry JD. Sex and Race Differences in Lifetime risk of heart failure with preserved ejection fraction and heart failure with reduced ejection fraction. *Circulation*. 2018;137:1814–1823.

18. Carmel S. Health and Well-Being in Late Life: Gender Differences Worldwide. *Front Med (Lausanne)*. 2019;6:218.

19. Gottdiener JS, McClelland RL, Marshall R, Shemanski L, Furberg CD, Kitzman DW, Cushman M, Polak J, Gardin JM, Gersh BJ, Aurigemma GP, Manolio TA. Outcome of congestive heart failure in elderly persons: influence of left ventricular systolic function. The Cardiovascular Health Study. *Ann Intern Med*. 2002;137:631–639.

20. Lee DS, Gona P, Vasan RS, Larson MG, Benjamin EJ, Wang TJ, Tu JV, Levy D. Relation of disease pathogenesis and risk factors to heart failure with preserved or reduced ejection fraction: insights from the framingham heart study of the national heart, lung, and blood institute. *Circulation*. 2009;119:3070–3077.

21. Mr Z, Cf B, Js I, Re S, Pj N, Ad B, R S, Bm P, P VB, M M, Mm R, Da B, Hl G, Mm L. Myocardial stiffness in patients with heart failure and a preserved ejection fraction: contributions of collagen and titin. *Circulation*. 2015;131. doi:10.1161/CIRCULATIONAHA.114.013215.

22. Franssen C, González Miqueo A. The role of titin and extracellular matrix remodelling in heart failure with preserved ejection fraction. *Neth Heart J*. 2016;24:259–267.

23. Kanagala P, Cheng ASH, Singh A, Khan JN, Gulsin GS, Patel P, Gupta P, Arnold JR, Squire IB, Ng LL, McCann GP. Relationship Between Focal and Diffuse Fibrosis Assessed by CMR and Clinical Outcomes in Heart Failure With Preserved Ejection Fraction. *JACC Cardiovasc Imaging*. 2019;12:2291–2301.

24. Kim GH, Uriel N, Burkhoff D. Reverse remodelling and myocardial recovery in heart failure. *Nat Rev Cardiol*. 2018;15:83–96.

25. Sweeney M, Corden B, Cook SA. Targeting cardiac fibrosis in heart failure with preserved ejection fraction: mirage or miracle? *EMBO Mol Med*. 2020;12:e10865.

26. Kusindarta DL, Wihadmadyatami H. The Role of Extracellular Matrix in Tissue Regeneration. IntechOpen; 2018. doi:10.5772/intechopen.75728.

27. Asgari M, Latifi N, Heris HK, Vali H, Mongeau L. In vitro fibrillogenesis of tropocollagen type III in collagen type I affects its relative fibrillar topology and mechanics. *Sci Rep*. 2017;7:1392.

28. Banerjee I, Fuseler JW, Price RL, Borg TK, Baudino TA. Determination of cell types and numbers during cardiac development in the neonatal and adult rat and mouse. *Am J Physiol Heart Circ Physiol*. 2007;293:H1883-1891.

29. Parisi L, Toffoli A, Ghezzi B, Mozzoni B, Lumetti S, Macaluso GM. A glance on the role of fibronectin in controlling cell response at biomaterial interface. *Jpn Dent Sci Rev*. 2020;56:50–55.

30. Zhong C, Chrzanowska-Wodnicka M, Brown J, Shaub A, Belkin AM, Burridge K. Rho-mediated contractility exposes a cryptic site in fibronectin and induces fibronectin matrix assembly. *J Cell Biol*. 1998;141:539–551.

31. McDonald JA, Kelley DG, Broekelmann TJ. Role of fibronectin in collagen deposition: Fab' to the gelatin-binding domain of fibronectin inhibits both fibronectin and collagen organization in fibroblast extracellular matrix. *J Cell Biol*. 1982;92:485–492.

32. Valiente-Alandi I, Potter SJ, Salvador AM, Schafer AE, Schips T, Carrillo-Salinas F, Gibson AM, Nieman ML, Perkins C, Sargent MA, Huo J, Lorenz JN, DeFalco T, Molkentin JD, Alcaide P, Blaxall BC. Inhibiting Fibronectin Attenuates Fibrosis and Improves Cardiac Function in a Model of Heart Failure. *Circulation*. 2018;138:1236–1252.

33. Treibel TA, López B, González A, Menacho K, Schofield RS, Ravassa S, Fontana M, White SK, DiSalvo C, Roberts N, Ashworth MT, Díez J, Moon JC. Reappraising myocardial fibrosis in severe aortic stenosis: an invasive and non-invasive study in 133 patients. *Eur Heart J*. 2018;39:699–709.

34. Zhang X, Stewart JA, Kane ID, Massey EP, Cashatt DO, Carver WE. Effects of elevated glucose levels on interactions of cardiac fibroblasts with the extracellular matrix. *In Vitro Cell Dev Biol Anim*. 2007;43:297–305.

35. Gu X, Fang T, Kang P, Hu J, Yu Y, Li Z, Cheng X, Gao Q. Effect of ALDH2 on High Glucose-Induced Cardiac Fibroblast Oxidative Stress, Apoptosis, and Fibrosis. *Oxid Med Cell Longev*. 2017;2017:9257967.

36. Medzikovic L, Aryan L, Eghbali M. Connecting sex differences, estrogen signaling, and microRNAs in cardiac fibrosis. *J Mol Med (Berl)*. 2019;97:1385–1398.

37. Schorb W, Conrad KM, Singer HA, Dostal DE, Baker KM. Angiotensin II is a potent stimulator of MAP-kinase activity in neonatal rat cardiac fibroblasts. *J Mol Cell Cardiol*. 1995;27:1151–1160.

38. Somanna NK, Yariswamy M, Garagliano JM, Siebenlist U, Mummidi S, Valente AJ, Chandrasekar B. Aldosterone-induced cardiomyocyte growth, and fibroblast migration and proliferation are mediated by TRAF3IP2. *Cell Signal*. 2015;27:1928–1938.

39. Meng X-M, Nikolic-Paterson DJ, Lan HY. TGF-β: the master regulator of fibrosis. *Nat Rev Nephrol*. 2016;12:325–338.

40. Marchese V, Juarez J, Patel P, Hutter-Lobo D. Density-Dependent ERK MAPK expression regulates MMP-9 and influences growth. *Mol Cell Biochem*. 2019;456:115–122.

41. Zheng L, Huang Y, Song W, Gong X, Liu M, Jia X, Zhou G, Chen L, Li A, Fan Y. Fluid shear stress regulates metalloproteinase-1 and 2 in human periodontal ligament cells: Involvement of extracellular signal-regulated kinase (ERK) and P38 signaling pathways. *Journal of Biomechanics*. 2012;45:2368–2375.

42. Krebber MM, van Dijk CGM, Vernooij RWM, Brandt MM, Emter CA, Rau CD, Fledderus JO, Duncker DJ, Verhaar MC, Cheng C, Joles JA. Matrix Metalloproteinases and Tissue Inhibitors of Metalloproteinases in Extracellular Matrix Remodeling during Left Ventricular Diastolic Dysfunction and Heart Failure with Preserved Ejection Fraction: A Systematic Review and Meta-Analysis. *Int J Mol Sci*. 2020;21:6742.

43. Liu P, Sun M, Sader S. Matrix metalloproteinases in cardiovascular disease. *Can J Cardiol*. 2006;22:25B-30B.

44. Visse R, Nagase H. Matrix Metalloproteinases and Tissue Inhibitors of Metalloproteinases. *Circulation Research*. 2003;92:827–839.

45. DeLeon-Pennell KY, Meschiari CA, Jung M, Lindsey ML. Matrix Metalloproteinases in Myocardial Infarction and Heart Failure. *Prog Mol Biol Transl Sci*. 2017;147:75–100.

46. Krebber MM, van Dijk CGM, Vernooij RWM, Brandt MM, Emter CA, Rau CD, Fledderus JO, Duncker DJ, Verhaar MC, Cheng C, Joles JA. Matrix Metalloproteinases and Tissue Inhibitors of Metalloproteinases in Extracellular Matrix Remodeling during Left Ventricular Diastolic Dysfunction and Heart Failure with Preserved Ejection Fraction: A Systematic Review and Meta-Analysis. *Int J Mol Sci*. 2020;21:E6742.

47. Heinzel FR, Hegemann N, Hohendanner F, Primessnig U, Grune J, Blaschke F, de Boer RA, Pieske B, Schiattarella GG, Kuebler WM. Left ventricular dysfunction in heart failure with preserved ejection fraction—molecular mechanisms and impact on right ventricular function. *Cardiovasc Diagn Ther*. 2020;10:1541–1560.

48. Gorter TM, Hoendermis ES, van Veldhuisen DJ, Voors AA, Lam CSP, Geelhoed B, Willems TP, van Melle JP. Right ventricular dysfunction in heart failure with preserved ejection fraction: a systematic review and meta-analysis. *Eur J Heart Fail*. 2016;18:1472–1487.

49. Kelly SC, Rau CD, Ouyang A, Thorne PK, Olver TD, Edwards JC, Domeier TL, Padilla J, Grisanti LA, Fleenor BS, Wang Y, Rector RS, Emter CA. The right ventricular transcriptome signature in Ossabaw swine with cardiometabolic heart failure: implications for the coronary vasculature. *Physiol Genomics*. 2021;53:99–115.

50. Aschauer S, Zotter-Tufaro C, Duca F, Kammerlander A, Dalos D, Mascherbauer J, Bonderman D. Modes of death in patients with heart failure and preserved ejection fraction. *International Journal of Cardiology*. 2017;228:422–426.

51. Oken DE, Boucek RJ. Quantitation of Collagen in Human Myocardium. *Circulation Research*. 1957;5:357–361.

52. Kadler KE, Hill A, Canty-Laird EG. Collagen fibrillogenesis: fibronectin, integrins, and minor collagens as organizers and nucleators. *Curr Opin Cell Biol*. 2008;20:495–501.

53. Krittanawong C, Virk HUH, Bangalore S, Wang Z, Johnson KW, Pinotti R, Zhang H, Kaplin S, Narasimhan B, Kitai T, Baber U, Halperin JL, Tang WHW. Machine learning prediction in cardiovascular diseases: a meta-analysis. *Sci Rep*. 2020;10:16057.

54. Krittanawong C, Zhang H, Wang Z, Aydar M, Kitai T. Artificial Intelligence in Precision Cardiovascular Medicine. *J Am Coll Cardiol*. 2017;69:2657–2664.

55. Krittanawong C, Johnson KW, Rosenson RS, Wang Z, Aydar M, Baber U, Min JK, Tang WHW, Halperin JL, Narayan SM. Deep learning for cardiovascular medicine: a practical primer. *Eur Heart J*. 2019;40:2058–2073.

56. Shah SJ, Katz DH, Selvaraj S, Burke MA, Yancy CW, Gheorghiade M, Bonow RO, Huang C-C, Deo RC. Phenomapping for Novel Classification of Heart Failure With Preserved Ejection Fraction. *Circulation*. 2015;131:269–279.

57. Lopatkin AJ, Collins JJ. Predictive biology: modelling, understanding and harnessing microbial complexity. *Nat Rev Microbiol*. 2020;18:507–520.

58. Baldi P, Brunak S, Chauvin Y, Andersen CA, Nielsen H. Assessing the accuracy of prediction algorithms for classification: an overview. *Bioinformatics*. 2000;16:412–424.

59. Lever J, Krzywinski M, Altman N. Classification evaluation. *Nature Methods*. 2016;13:603–604.

60. Lever J, Krzywinski M, Altman N. Model selection and overfitting. *Nature Methods*. 2016;13:703–704.

61. Shao J. Linear Model Selection by Cross-validation. *Journal of the American Statistical Association*. 1993;88:486–494.

62. Natekin A, Knoll A. Gradient boosting machines, a tutorial. *Front Neurorobot*. 2013;7:21.

63. Yao X. Evolving artificial neural networks. *Proceedings of the IEEE*. 1999;87:1423–1447.

64. Haglin JM, Jimenez G, Eltorai AEM. Artificial neural networks in medicine. *Health Technol*. 2019;9:1–6.

65. Marinucci D, Sbrollini A, Marcantoni I, Morettini M, Swenne CA, Burattini L. Artificial Neural Network for Atrial Fibrillation Identification in Portable Devices. *Sensors (Basel)*. 2020;20:E3570.

66. Itchhaporia D, Snow PB, Almassy RJ, Oetgen WJ. Artificial neural networks: current status in cardiovascular medicine. *J Am Coll Cardiol*. 1996;28:515–521.

67. Papik K, Molnar B, Schaefer R, Dombovari Z, Tulassay Z, Feher J. Application of neural networks in medicine - a review. *Med Sci Monit*. 1998;4:MT538–MT546.

68. Jain AK, Mao J, Mohiuddin KM. Artificial neural networks: a tutorial. *Computer*. 1996;29:31–44.

69. Tokar AS, Johnson PA. Rainfall-Runoff Modeling Using Artificial Neural Networks. *Journal of Hydrologic Engineering*. 1999;4:232–239.

70. Tu JV. Advantages and disadvantages of using artificial neural networks versus logistic regression for predicting medical outcomes. *J Clin Epidemiol*. 1996;49:1225–1231.

71. Hinton GE. Connectionist Learning Procedures. *Artif Intell*. 1989. doi:10.1016/0004-3702(89)90049-0.

72. Dixon JA, Spinale FG. Large Animal Models of Heart Failure. *Circulation: Heart Failure*. 2009;2:262–271.

73. Riehle C, Bauersachs J. Small animal models of heart failure. *Cardiovascular Research*. 2019;115:1838–1849.

74. Spannbauer A, Traxler D, Zlabinger K, Gugerell A, Winkler J, Mester-Tonczar J, Lukovic D, Müller C, Riesenhuber M, Pavo N, Gyöngyösi M. Large Animal Models of Heart Failure With Reduced Ejection Fraction (HFrEF). *Frontiers in Cardiovascular Medicine*. 2019;6. Available at https://www.frontiersin.org/article/10.3389/fcvm.2019.00117. Accessed March 7, 2022.

75. Olver TD, Edwards JC, Jurrissen TJ, Veteto AB, Jones JL, Gao C, Rau C, Warren CM, Klutho PJ, Alex L, Ferreira -Nichols Stephanie C., Ivey JR, Thorne PK, McDonald KS, Krenz M, Baines CP, Solaro RJ, Wang Y, Ford DA, Domeier TL, Padilla J, Rector RS, Emter CA. Western Diet-Fed, Aortic-Banded Ossabaw Swine. *JACC: Basic to Translational Science*. 2019;4:404–421.

76. Lourenço AP, Leite-Moreira AF, Balligand J-L, Bauersachs J, Dawson D, de Boer RA, de Windt LJ, Falcão-Pires I, Fontes-Carvalho R, Franz S, Giacca M, Hilfiker-Kleiner D, Hirsch E, Maack C, Mayr M, Pieske B, Thum T, Tocchetti CG, Brutsaert DL, Heymans S. An integrative translational approach to study heart failure with preserved ejection fraction: a position paper from the Working Group on Myocardial Function of the European Society of Cardiology. *Eur J Heart Fail*. 2018;20:216–227.

77. Obokata M, Reddy YNV, Borlaug BA. Diastolic Dysfunction and Heart Failure With Preserved Ejection Fraction: Understanding Mechanisms by Using Noninvasive Methods. *JACC Cardiovasc Imaging*. 2020;13:245–257.

78. Zhang J, Gajjala S, Agrawal P, Tison GH, Hallock LA, Beussink-Nelson L, Lassen MH, Fan E, Aras MA, Jordan C, Fleischmann KE, Melisko M, Qasim A, Shah SJ, Bajcsy R, Deo RC. Fully Automated Echocardiogram Interpretation in Clinical Practice. *Circulation*. 2018;138:1623–1635.

79. McCulloch AD. Systems Biophysics: Multiscale Biophysical Modeling of Organ Systems. *Biophys J*. 2016;110:1023–1027.

80. Olver TD, Hiemstra JA, Edwards JC, Schachtman TR, Heesch CM, Fadel PJ, Laughlin MH, Emter CA. Loss of Female Sex Hormones Exacerbates Cerebrovascular and Cognitive Dysfunction in Aortic Banded Miniswine Through a Neuropeptide Y–Ca2+-Activated Potassium Channel–Nitric Oxide Mediated Mechanism. *J Am Heart Assoc*. 2017;6:e007409.

81. Swindle MM. Surgery, anesthesia, and experimental techniques in swine. Iowa State University Press; 1998. Available at https://scholar.google.com/scholar_lookup?title=Surgery%2C+anesthesia%2C+and+experimental+techniques+in+swine&author=Swindle%2C+M.+Michael.&publication_year=1998. Accessed February 8, 2022.

82. Olver TD, Edwards JC, Jurrissen TJ, Veteto AB, Jones JL, Gao C, Rau C, Warren CM, Klutho PJ, Alex L, Ferreira-Nichols SC, Ivey JR, Thorne PK, McDonald KS, Krenz M, Baines CP, Solaro RJ, Wang Y, Ford DA, Domeier TL, Padilla J, Rector RS, Emter CA. Western Diet-Fed, Aortic-Banded Ossabaw Swine: A Preclinical Model of Cardio-Metabolic Heart Failure. *JACC Basic Transl Sci*. 2019;4:404–421.

83. Marshall KD, Muller BN, Krenz M, Hanft LM, McDonald KS, Dellsperger KC, Emter CA. Heart failure with preserved ejection fraction: chronic low-intensity interval exercise training preserves myocardial O2 balance and diastolic function. *J Appl Physiol (1985)*. 2013;114:131–147.

84. Livak KJ, Schmittgen TD. Analysis of Relative Gene Expression Data Using Real-Time Quantitative PCR and the 2−ΔΔCT Method. *Methods*. 2001;25:402–408.

85. Emter CA, Bowles DK. STORE-OPERATED CA 2+ ENTRY IS NOT ESSENTIAL FOR PDGF-BB INDUCED PHENOTYPE MODULATION IN RAT AORTIC SMOOTH MUSCLE. *Cell Calcium*. 2010;48:10–18.

86. A new twist on an old idea part 2: cyclosporine preserves normal mitochondrial but not cardiomyocyte function in mini-swine with compensated heart failure - PubMed. Available at https://pubmed.ncbi.nlm.nih.gov/24963034/. Accessed February 9, 2022.

87. Toth M, Fridman R. Assessment of Gelatinases (MMP-2 and MMP-9 by Gelatin Zymography. *Methods Mol Med*. 2001;57:163–174.

88. Kang H. The prevention and handling of the missing data. *Korean J Anesthesiol*. 2013;64:402–406.

89. Kang H. The prevention and handling of the missing data. *Korean J Anesthesiol*. 2013;64:402–406.

90. Tresp V, Ahmad S, Neuneier R. Training Neural Networks with Deficient Data. In: Advances in Neural Information Processing Systems. Morgan-Kaufmann; 1993. Available at https://proceedings.neurips.cc/paper/1993/hash/a8ecbabae151abacba7dbde04f761c37-Abstract.html. Accessed February 24, 2022.

91. Sharpe PK, Solly RJ. Dealing with missing values in neural network-based diagnostic systems. *Neural Comput & Applic*. 1995;3:73–77.

92. Pigott TD. A Review of Methods for Missing Data. *Educational Research and Evaluation*. 2001;7:353–383.

93. Taljaard M, Donner A, Klar N. Imputation Strategies for Missing Continuous Outcomes in Cluster Randomized Trials. *Biometrical Journal*. 2008;50:329–345.

94. Little RJA, Rubin DB. Statistical Analysis with Missing Data. John Wiley & Sons; 2019: 1-462.

95. Olinsky A, Chen S, Harlow L. The comparative efficacy of imputation methods for missing data in structural equation modeling. *European Journal of Operational Research*. 2003;151:53–79.

96. Doherty KAJ, Adams RG, Davey N. Non Euclidean Norms and Data Normalisation. 2004;:6.

97. KumarSingh B, Verma K, S. Thoke A. Investigations on Impact of Feature Normalization Techniques on Classifier's Performance in Breast Tumor Classification. *IJCA*. 2015;116:11–15.

98. Jayalakshmi T, Santhakumaran A. Statistical Normalization and Back Propagationfor Classification. *IJCTE*. 2011;:89–93.

99. Jain AK, Mao J, Mohiuddin KM. Artificial Neural Networks: A Tutorial. *Computer*. 1996;29:31–44.

100. Basheer IA, Hajmeer M. Artificial neural networks: fundamentals, computing, design, and application. *J Microbiol Methods*. 2000;43:3–31.

101. van der Smagt P. Minimisation Methods for Training Feed-Forward Neural Networks. *Neural Networks*. 1996;7:1–11.

102. Deng X, Liu Q, Deng Y, Mahadevan S. An improved method to construct basic probability assignment based on the confusion matrix for classification problem. *Information Sciences*. 2016;340–341:250–261.

103. Goutte C, Gaussier E. A Probabilistic Interpretation of Precision, Recall and F-Score, with Implication for Evaluation. In: Losada DE, Fernández-Luna JM, eds. Advances in Information Retrieval. Berlin, Heidelberg: Springer; 2005: 345–359.

104. Pedram A, Razandi M, Narayanan R, Dalton JT, McKinsey TA, Levin ER. Estrogen regulates histone deacetylases to prevent cardiac hypertrophy. *Mol Biol Cell*. 2013;24:3805–3818.

105. Morselli E, Santos RS, Criollo A, Nelson MD, Palmer BF, Clegg DJ. The effects of oestrogens and their receptors on cardiometabolic health. *Nat Rev Endocrinol*. 2017;13:352–364.

106. Ferreira C, Trindade F, Ferreira R, Neves JS, Leite-Moreira A, Amado F, Santos M, Nogueira-Ferreira R. Sexual dimorphism in cardiac remodeling: the molecular mechanisms ruled by sex hormones in the heart. *J Mol Med*. 2022;100:245–267.

107. Dubey RK, Gillespie DG, Jackson EK, Keller PJ. 17β-Estradiol, Its Metabolites, and Progesterone Inhibit Cardiac Fibroblast Growth. *Hypertension*. 1998;31:522–528.

108. Lim GB. Progesterone receptor controls heart maturation. *Nat Rev Cardiol*. 2021;18:387–387.

109. Thomas P, Pang Y. Protective actions of progesterone in the cardiovascular system: Potential role of membrane progesterone receptors (mPRs) in mediating rapid effects. *Steroids*. 2013;78:583–588.

110. de Souza RR. Aging of myocardial collagen. *Biogerontology*. 2002;3:325–335.

111. Cypen J, Ahmad T, Testani JM, DeVore AD. Novel Biomarkers for the Risk Stratification of Heart Failure with Preserved Ejection Fraction. *Curr Heart Fail Rep*. 2017;14:434–443.

112. Chirinos JA, Orlenko A, Zhao L, Basso MD, Cvijic ME, Li Z, Spires TE, Yarde M, Wang Z, Seiffert DA, Prenner S, Zamani P, Bhattacharya P, Kumar A, Margulies KB, Car BD, Gordon DA, Moore JH, Cappola TP. Multiple Plasma Biomarkers for Risk Stratification in Patients With Heart Failure and Preserved Ejection Fraction. *Journal of the American College of Cardiology*. 2020;75:1281–1295.

113. Ward M, Yeganegi A, Baicu CF, Bradshaw AD, Spinale FG, Zile MR, Richardson WJ. Ensemble machine learning model identifies patients with HFpEF from matrix-related plasma biomarkers. *American Journal of Physiology-Heart and Circulatory Physiology*. 2022;322:H798–H805.

114. Wu C-K, Su M-YM, Wu Y-F, Hwang J-J, Lin L-Y. Combination of Plasma Biomarkers and Clinical Data for the Detection of Myocardial Fibrosis or Aggravation of Heart Failure Symptoms in Heart Failure with Preserved Ejection Fraction Patients. *Journal of Clinical Medicine*. 2018;7:427.

115. Dzeshka MS, Shantsila E, Snezhitskiy VA, Lip GYH. Circulating biomarkers of myocardial fibrosis and cellular apoptosis in patients with atrial fibrillation and heart failure with preserved ejection fraction. *European Heart Journal*. 2019;40:ehz745.0635.

116. Fritsch S, Guenther F, Guenther MF. Package 'neuralnet.' *Training of Neural Networks*. 2019.

Supplementary material

Artificial neural network code

#Loading necessary packages

```
library("neuralnet")

library("caret")
```

#preprocessing

removing subjects with incomplete data (that cannot be imputed)

```
dat <- dat[-c(7, 20, 27), ]

View(dat)
```

Replacing any missing values with NA

```
dat <- replace(dat, dat == 0, NA)
```

#finding missing data

```
#apply(is.na(dat), 2, which)
```

#Within group mean imputation

```
dat$DUSP4_18S1e5_mr_RV<-
ave(dat$DUSP4_18S1e5_mr_RV,dat$group,FUN=function(x)
  ifelse(is.na(x), mean(x,na.rm=TRUE), x))

dat$ColI_18S1e5_mr._LV<-ave(dat$ColI_18S1e5_mr._LV,dat$group,FUN=function(x)
  ifelse(is.na(x), mean(x,na.rm=TRUE), x))

dat$Col_ug.mg_pr_LV <-ave(dat$Col_ug.mg_pr_LV,dat$group,FUN=function(x)
  ifelse(is.na(x), mean(x,na.rm=TRUE), x))
```

#Testing existence of any missing values

```
test <- length(TRUE[is.na(dat)])
test
```

#Min-max normalization

```
## all values normalized
normalize <- function(x)
{
  return((x- min(x)) /(max(x)-min(x)))
```

```
}
```

#Replacing the data with the normalized values

```
dat[3:length(dat)] <- as.data.frame(lapply(dat[3:length(dat)], normalize))

View(dat)
```

#One way ANOVA

#Setting experimental groups as levels

```
levels(dat$group) <- dat[1]
```

#Identifying the independent variable (experimental groups status)

```
dat$group <- as.factor(dat$group)
```

#Setting the experimental groups status as factor

```
is.factor(dat$group)

dat$group
```

#Extraction of variable names from dataset

```
ind_var1 <- colnames(dat)[unlist(sapply(2:ncol(dat), function(i)

if(length(unique(dat[,i]))>20) return(i)))]

ind_var1 <- ind_var1[2:97]
```

```
print(ind_var1)
```

#Setting lists to store results

```
pvalue_anova <- NULL

model_matrix <- NULL
```

#ANOVA

```
for (i in ind_var1){

  #model <- lm(i ~ dat$group, data = dat)

  model <- lm(as.formula(paste0("`",i,"`~",paste0("dat$group", collapse = "+"))),
data=dat)

  sumres <- summary(model)

  pvalue_anova <- pf(sumres$fstatistic[1L], sumres$fstatistic[2L], sumres$fstatistic[3L],
lower.tail = FALSE)

  model_matrix <- rbind(model_matrix, pvalue_anova)

}

model_matrix <- t(model_matrix)

model_matrix <- data.frame(variable = ind_var1,

                           pvalue_anova = as.numeric(model_matrix))
```

```
View(model_matrix)
```

#Preparing variables for ANN

#Subset of the dataset with only the predictors

```
dats <- data.frame(dat$group, dat$Col_ug.mg_pr_LV, dat$Col_ug.mg_pr_RV,
            dat$TIMP1_18S1e5_mr._LV, dat$ColIII_18S1e5_mr_RV, dat$JNK_pr._LV,
            dat$MMP14_ACTIVITY_LV_90, dat$MMP2_activity_LV,
            dat$ColI_18S1e5_mr_RV,  dat$ColI_18S1e5_mr._LV)
colnames(dats) <- c("group", "Col_ug.mg_pr_LV", "Col_ug.mg_pr_RV",
          "TIMP1_18S1e5_mr._LV",  "ColIII_18S1e5_mr_RV", "JNK_pr._LV",
          "MMP14_ACTIVITY_LV_90",  "MMP2_activity_LV", "ColI_18S1e5_mr_RV",
          "ColI_18S1e5_mr._LV")
View(dats)
```

#Setting input variables for the ANN

```
names <- colnames(dats[-1])
```

#Setting 4 fold cross validation

```
K <- 4
```

```
index <- 1:nrow(dats)

for(i in 1:length(unique(dats$group))){

 i_loc <- which(dats$group==unique(dats$group)[i])

 set.seed(i)

 folds <- caret::createFolds(1:length(i_loc),4)

 for (j in 1:K) {

  index[i_loc[unlist(folds[j])]] <- j

 }

}
```

#Modeling

```
confusion_list <- rep(list(matrix(NA,4,4)),5)

acc <- NULL

f1score <- NULL

bacc <- NULL

layer1 <- 8

layer2 <- 5
```

#ANN using neuralnet package

```
for(k in 1:K){
  test_<-dats[which(index==k),]
  train_ <- dats[-which(index==k),]
  f <- as.formula(paste("group ~", paste(names, collapse = " + ")))

  for (l in layer1) {
    for (h in layer2){

      set.seed(12345)
      nn <- neuralnet(f,data=train_ ,hidden= c(l,h) ,act.fct = "logistic", linear.output =
FALSE,
           stepmax =    1e+11)
      plot(nn)
```

#Transforming model prediction into 0, 1 format for the confusion matrix using base R

```
      pred <- predict(nn, test_)
      pred_label <- names(table(unique(test_$group)))[apply(pred, 1, which.max)]
```

```
    confusion_list[[k]] <- table(test_$group, pred_label)
    print(confusion_list[[k]])
    #Using caret package confusion matrix function
    #Setting the experimental groups and predicted groups as ordered factors
    pred_label <- as.factor(pred_label)
    pred_label <- ordered(pred_label, levels = c("Con-Int", "AB-Int", "Con-OVX", "AB-
OVX"))
    test_$group <- ordered(test_$group, levels = c("Con-Int", "AB-Int", "Con-OVX",
"AB-OVX"))
   #Storing confusion matrices into cm variable
    cm <- confusionMatrix(pred_label, test_$group)
    print(cm)
    #Extraction of accuracy stores from each fold and storing them in separate
dataframes
    acc<- rbind(cm$overall['Accuracy'], acc)
    f1score <- rbind(cm[["byClass"]][ , "F1"], f1score)
    bacc <- rbind(cm[["byClass"]][, "Balanced Accuracy"], bacc)
  }
 }
```

```
}


#Mean percentage accuracy

print(mean(acc))


#Averaged F1 score per fold then across all folds

F1sc <- NULL

F1sc <- rbind(rowMeans(f1score, na.rm = TRUE))

print(mean(F1sc))


#Balanced accuracy for each experimental group averaged across the folds

print(bacc)

balac <- rbind(colMeans(bacc, na.rm = TRUE))

print(balac)


#Custom Activation function equation for softmax

softmax = custom <- function(x) {log(1+exp(x))}
```

#Logistic, tanh, and RelU are available as part of neuralnet package in R.

More information can be found in [116]

ECM component variables quantified in both Right Ventricle and left ventricle and type of quantification through qPCR, Western Blot, and Zymography				
Category	**Variable name**	**mRNA**	**Protein**	**Activity and/ or abundance**
ECM structural proteins	Total collagen content		✓	
	Collagen subtype I	✓		
	Collagen subtype III	✓		
	Fibronectin	✓	✓	
Matrix Metalloproteases	MMP1	✓		
	MMP2	✓		✓
	MMP3	✓		
	MMP9	✓		✓
	MMP13	✓		
	MMP14	✓	✓	✓
Tissue inhibitors of Matrix Metalloproteases	TIMP1	✓		
	TIMP2	✓	✓	
	TIMP4	✓		
Mitogen activated protein Kinases	MAPK1	✓		
	MAPK3	✓		
	MAPK8	✓		
	MAPK9	✓		
Mitogen activated protein Kinase Kinases	MAP2K1	✓		
	MAP2K2	✓		
	MAP2K4	✓		
	MAP2K7	✓		
Extracellular signal-regulated Kinase	ERK		✓	
	Phosphorylated ERK		✓	
	Phosphorylated ERK/ERK		✓	

c-Jun Amino-Terminal Kinases	JNK		✓	
	Phosphorylated JNK		✓	
	Phosphorylated JNK/JNK		✓	
Dual-Specificity Phosphatases	DUSP1	✓		
	DUSP4	✓		
	DUSP6	✓		
	DUSP9	✓		
	DUSP10	✓		
Sex hormone receptors	Estrogen Receptor 1	✓	✓	
	Estrogen Receptor 2	✓	✓	
	Progesterone Receptor	✓		
	Progesterone Receptor - Isoform A		✓	
	Progesterone Receptor - Isoform B		✓	
	progesterone receptor - membrane component 1	✓	✓	

Table s-1 : A list of all quantified extracellular matrix components